

Running header: Topography of scene memory and perception activity

1 Topography of scene memory and perception activity in 2 posterior cortex – a publicly available resource

3

4 Adam Steel^{1,2,*}, Deepa Prasad³, Brenda D. Garcia⁴, Caroline E. Robertson³

5 ¹Department of Psychology, University of Illinois

6 ²Beckman Institute for Advanced Science and Technology, University of Illinois

7 ³Department of Psychology, Dartmouth College

8 ⁴University of California San Diego Medical School, University of California San Diego

9 *Corresponding author: adamdanielsteel@gmail.com

10

11 Competing interests: The authors declare no competing interests.

12 Data availability: Probabilistic parcels and fMRI localizer tasks are available from <https://osf.io/xmhn7/>.

13 Other supporting data will be made available upon publication.

14 Code availability: This data does not use any original code. Any additional information required to reanalyze
15 the data reported in this paper is available from the lead contact upon request.

16

17 Acknowledgements: This work was supported by an award from the National Institutes of Mental Health
18 (R01MH130529) to CER. AS was supported by the Neukom Institute for Computational Sciences.

19

20 Number of Figures: 11

21 Number of Tables: 1

22 Abstract word count: 285

23 Introduction/Discussion text word count: 883/2398

24 Author contributions: AS and CER designed the research. AS, DP, BDG collected and processed the data.
25 AS analyzed the data. AS and CER wrote the manuscript. All authors reviewed and edited the manuscript.

26 During the preparation of this work, the author(s) used Claude (Anthropic) to assist in revising the
27 manuscript. After using this tool/service, the author(s) reviewed and edited the content as needed and
28 take(s) full responsibility for the content of the publication.

29

30 Abstract

31 Adaptive behavior in complex environments requires integrating visual perception with
32 memory of our spatial environment. Recent work has implicated three brain areas in
33 posterior cerebral cortex — the place memory areas (PMAs) that are anterior to the three
34 visual scene perception areas (SPAs) – in this function. However, PMAs’ relationship to the
35 broader cortical hierarchy remains unclear due to limited group-level characterization. Here,
36 we examined the PMA and SPA locations across three fMRI datasets (44 participants, 29
37 female). SPAs were identified using a standard visual localizer where participants viewed
38 scenes versus faces. PMAs were identified by contrasting activity when participants recalled
39 personally familiar places versus familiar faces (Datasets 1-2) or places versus multiple
40 categories (familiar faces, bodies, and objects, and famous faces; Dataset 3). Across
41 datasets, the PMAs were located anterior to the SPAs on the ventral and lateral cortical
42 surfaces. The anterior displacement between PMAs and SPAs was highly reproducible.
43 Compared to public atlases, the PMAs fell at the boundary between externally-oriented
44 networks (dorsal attention) and internally-oriented networks (default mode). Additionally,
45 while SPAs overlapped with retinotopic maps, the PMAs were consistently located anterior
46 to mapped visual cortex. These results establish the anatomical position of the PMAs at
47 inflection points along the cortical hierarchy between unimodal sensory and transmodal,
48 apical regions, which informs broader theories of how the brain integrates perception and
49 memory for scenes. We have released probabilistic parcels of these regions to facilitate
50 future research into their roles in spatial cognition.

51 Significance statement

52 Complex behavior requires the dynamic interplay between mnemonic and perceptual
53 information. For example, navigation requires representation of the current visual scene and
54 its relationship to the surrounding visuospatial context. We have suggested that the place
55 memory areas, three brain areas located anterior to the scene perception areas in visual
56 cortex, are well-positioned to serve this role. Here, in a large group of participants, we show
57 that the place memory areas are robustly localizable, and that their position at the interface
58 of multiple distributed brain networks is uniquely suited to mnemonic-perceptual
59 integration. We have released probabilistic regions-of-interest and localization procedure so
60 that others can identify these areas in their own participants.

61 Introduction

62 The integration of perception and memory is a fundamental challenge for the brain, requiring
63 neural systems to simultaneously maintain current sensory input while accessing relevant
64 stored information (Rust and Palmer, 2021). This integration is particularly evident during
65 spatial navigation, where we dynamically exchange information between the immediate
66 visual scene and memory of the broader environment to interpret visible features, predict
67 unseen elements, and guide attentional and motor decisions (Robertson et al., 2016; Brunec
68 et al., 2018; Haskins et al., 2020; Berens et al., 2021; Draschkow et al., 2022). Understanding
69 how the brain's functional architecture enables perceptual and mnemonic representations
70 to effectively interface, while also avoiding interference, is therefore a central question in
71 cognitive neuroscience (Summerfield and De Lange, 2014; Kiyonaga et al., 2017; Favila et al.,
72 2020; Libby and Buschman, 2021).

73 Recent work has identified a network of three brain areas in posterior cerebral cortex that
74 may play a crucial role in bridging perception and memory in the domain of scenes (Steel et
75 al., 2021, 2023, 2024b). These "place memory areas" selectively activate when individuals
76 recall familiar places (e.g., their house) compared to other memorable stimuli like familiar
77 people (e.g., their mother) (Steel et al., 2021). Critically, each place memory area is located
78 immediately anterior and adjacent to one of the three functionally-defined "scene
79 perception areas" in high-level visual cortex - the occipital place area (OPA),
80 parahippocampal place area (PPA), and medial place area (MPA, also known as retrosplenial
81 complex), on the brain's lateral, ventral, and medial surfaces, respectively (Epstein and
82 Kanwisher, 1998; Hasson et al., 2003; Epstein et al., 2007; Dilks et al., 2013; Silson et al.,
83 2016). This systematic topographical relationship suggests the place memory areas are
84 anatomically positioned to directly access perceptual representations of scenes (Steel et al.,
85 2023), which may change with age (Srokova et al., 2022).

86 Functionally, the place memory areas exhibit several key properties that highlight their role
87 in bridging perception and memory. The PMAs areas contain multivariate representations of
88 specific remembered scene views (Bainbridge et al., 2020; Steel et al., 2023), and activation
89 in these areas scales with the amount of remembered visuospatial context associated with
90 a viewed scene (Steel et al., 2023). Connectivity analyses show that the PMAs constitute a
91 distinct functional network from the SPAs, which is more strongly connected with spatial
92 memory structures like the hippocampus compared to early visual cortex (Baldassano et al.,
93 2016; Silson et al., 2016, 2019; Steel et al., 2021). Additionally, PMAs are dynamically
94 connected to SPAs through voxel-wise retinotopically opponent patterns during tasks
95 requiring perceptual-mnemonic interaction, such as recognizing familiar scenes (Steel et
96 al., 2024b, 2024a). Finally, the anterior shift of memory compared with perception may be

97 specific to scene stimuli as compared with faces (Steel et al., 2021; Chen et al., 2024). Taken
98 together, this organization aligns with a specialized role in processing out-of-view spatial
99 information during navigation (Steel et al., 2023).

100 While these properties make the place memory areas compelling candidates for integrating
101 perceptual and mnemonic representations of scenes, their broader relationship to large-
102 scale cortical topography remains unclear. This gap stems partly from methodological
103 choices in prior research. Given the individualized functional location of category-selective
104 areas in high-level visual cortex (Kanwisher et al., 1997; Epstein and Kanwisher, 1998; Grill-
105 Spector and Weiner, 2014; Kanwisher, 2017), most investigations have employed subject-
106 specific localization approaches to define these areas (Steel et al., 2021, 2023, 2024b;
107 Srokova et al., 2022), leaving open questions about whether the PMAs represent a
108 fundamental feature of human cortical organization or whether their location varies
109 substantially across individuals and methodological approaches. Additionally, because
110 group-level analyses have been limited, the place memory areas' relationships with other
111 known anatomical and functional landmarks (e.g., retinotopic maps (Wandell et al., 2007;
112 Wang et al., 2015) or large-scale cortical networks (Raichle et al., 2001; Fox et al., 2005;
113 Thomas Yeo et al., 2011; Yeo et al., 2015; Braga and Buckner, 2017; DiNicola et al., 2020; Du
114 et al., 2024) and functional gradients (Margulies et al., 2016; Huntenburg et al., 2018; Reznik
115 et al., 2024)) remain poorly characterized. Understanding these relationships can provide
116 important insight into the role of these memory areas in the brain outside of the visual
117 system and shed light on the relationship between spatial memory processes and broader
118 large-scale organizing principles of the human brain.

119 Here we address these open questions by characterizing the topography of place memory
120 areas across three independent datasets that vary in their fMRI acquisition parameters,
121 preprocessing approaches, and experimental designs. This approach allows us to establish
122 the consistency of these areas' locations relative to scene perception areas and other
123 cortical landmarks, while controlling for methodology-specific effects. Our results suggest
124 the place memory areas – each located immediately anterior to a classic scene perception
125 area on the ventral and dorsal surface of the human brain – represent a robust and consistent
126 feature of human functional cortical organization. Further, we establish their anatomical
127 position at inflection points along the cortical hierarchy between unimodal sensory and
128 transmodal, apical regions, which informs broader theories of how the brain integrates
129 perception and memory. Finally, we have made probabilistic parcels defining their locations
130 freely available to the research community to facilitate future research on these areas, and
131 to better understand their probabilistic relationship with reference to other probabilistic
132 atlases of functional areas in the human visual system (Julian et al., 2012; Wang et al., 2015;
133 Rosenke et al., 2021).

134

135 Methods

136 Procedure

137 The data for this study comprised functional localizers from three independent datasets.
138 Dataset 1 and Dataset 3 shared 3 participants, otherwise, all participants were non-
139 overlapping. Dataset 1 (Steel et al., 2021) and Dataset 2 (Steel et al., 2022, 2023, 2024b) were
140 analyzed for different studies that have been previously published. Dataset 3 was collected
141 for a separate study that has not been published.

142 The datasets in this study differed on their imaging parameters and task paradigms, which
143 enabled us to test the impact of these factors on the robustness of the place memory and
144 scene perception area location. Datasets 1 and 2 had different imaging parameters but
145 identical task paradigms. Datasets 2 and 3 had identical imaging parameters but different
146 task paradigms. Datasets 1 and 3 had different imaging parameters and task paradigms. A
147 general description of the relationships between these datasets is detailed in Table 1, and a
148 detailed description of all relevant details are reported below.

149 *Table 1. Relationship between Datasets 1-3.*

<i>Dataset</i>	<i>Number of participants</i>	<i>MRI acquisition / processing</i>	<i>Task conditions (imagery)</i>	<i>Publications</i>
<i>Dataset 1</i>	14	Single echo Standard	Familiar places Familiar faces	Steel et al., 2021
<i>Dataset 2</i>	23	Multi-echo ME-ICA	Familiar places Familiar faces	Steel et al., 2022; Steel et al., 2023; Steel*, Silson*, et al., 2024
<i>Dataset 3</i>	10 (3 shared with Dataset 1)	Multi-echo ME-ICA	Familiar places Familiar faces Familiar bodies Familiar objects Famous faces	Unpublished

150

151 Participants

152 Data from 44 unique participants (Age: 24.9±6.1 s.d., 15 male) comprise this study and are
153 distributed across three different datasets (Dataset 1: N = 14, Age: 25.6±4.1 s.d., 5 male;

154 Dataset 2: N = 23, Age: 24.6±7.7 s.d., 8 male; Dataset 3: N =10, Age: 25.8±3.3 s.d., 4 male).
155 Three participants were present in both Dataset 1 and Dataset 3. All subjects had normal or
156 correct to normal vision, were not colorblind, and were free from neurological or psychiatric
157 conditions. Written consent was obtained from all participants in accordance with the
158 Declaration of Helsinki and with a protocol and consent form approved by the Dartmouth
159 College Institutional Review Board (Protocol #31288). Participants were compensated for
160 their time at a rate of \$20/hr. No statistical methods were used to pre-determine sample
161 sizes.

162 Visual Stimuli and Tasks

163 Perception and memory tasks - Datasets 1 and 2

164 *Static scene perception area Localizer*

165 The scene perception areas (SPAs, i.e. occipital place area, OPA; parahippocampal place
166 area, PPA; medial place area, MPA) are regions that selectively activate when an individual
167 perceives places (i.e., a kitchen) compared with other categories of visual stimuli (i.e., faces,
168 objects, bodies) (Epstein and Kanwisher, 1998; Silson et al., 2016; Weiner et al., 2018; Steel
169 et al., 2021). To identify these areas in each person, participants performed an independent
170 functional localizer scan. On each run of the localizer (2 runs), participants passively viewed
171 blocks of scene, face, and object images presented in rapid succession (500 ms stimulus,
172 500 ms ISI). Blocks were 24 s long, and each run comprised 12 blocks (4 blocks/condition).
173 There was no interval between blocks.

174 *Place memory area Localizer*

175 The place memory areas (PMAs) are defined as regions that selectively activate when a
176 person recalls personally familiar places (i.e., their kitchen) compared with personally
177 familiar people (i.e., their mother)(Steel et al., 2021). To identify these areas in each person,
178 participants performed an independent functional localizer scan. Prior to fMRI scanning,
179 participants generated a list of 36 personally familiar people and places to establish
180 individualized stimuli (72 stimuli total). These stimuli were generated based on the following
181 instructions.

182 *“For your scan, you will be asked to visualize people and places that are personally*
183 *familiar to you. So, we need you to provide these lists for us. For personally familiar*
184 *people, please choose people that you know in real life (no celebrities) that you can*
185 *visualize in great detail. You do not need to be contact with these people now, as*
186 *long as you knew them personally and remember what they look like. So, you could*
187 *choose a childhood friend even if you are no longer in touch with this person.*
188 *Likewise, for personally familiar places, please list places that you have been to and*

189 *can richly visualize. You should choose places that are personally relevant to you,*
190 *so you should avoid choosing places that you have only been to one time. You*
191 *should not choose famous places where you have never been. You can choose*
192 *places that span your whole life, so you could do your current kitchen, as well as*
193 *the kitchen from your childhood home.”*

194 During fMRI scanning, participants recalled these people and places. On each trial,
195 participants saw the name of a person or place and recalled them in as much detail as
196 possible for the duration that the name appeared on the screen (10 s). Trials were separated
197 by a variable ISI (4-8 s). Place memory areas were localized by contrasting activity when
198 participants recalled personally familiar places compared with people (see ROI definitions
199 section). All trials were unique stimuli, and conditions (i.e., people or place stimuli) were
200 pseudo-randomly intermixed so that no more than two repeats per condition occurred in a
201 row.

202 **Memory task - Dataset 3**

203 Dataset 3 comprised two tasks, a multi-category dynamic perception task and a multi-
204 category dynamic memory task. The data from the multi-category perception task is being
205 reported in a separate publication and will not be discussed here.

206 *Multi-category place memory localizer*

207 Prior to fMRI scanning, participants generated a list of 5 examples from 5 categories:
208 personally familiar people’s faces (e.g., wife’s face, sister’s face), familiar people’s body
209 parts (e.g., mother’s hands, father’s feet), familiar places (e.g., my kitchen, college library),
210 familiar objects roughly the size of a person’s face (e.g., laptop, rugby ball), and famous
211 people’s faces (Beyonce’s face, Obama’s face) to establish individualized stimuli (72 stimuli
212 total). These stimuli were generated based on the following instructions.

213 *“For your scan, you will be asked to visualize people’s faces and bodies, places, and*
214 *objects that are familiar to you. So, we need you to provide these lists for us. For*
215 *personally familiar people’s faces, please choose people that you know in real life*
216 *(no celebrities) that you can visualize in great detail. You do not need to be contact*
217 *with these people now, as long as you knew them personally and remember what*
218 *they look like. So, you could choose a childhood friend even if you are no longer in*
219 *touch with this person.*

220 *For bodies, you will choose 5 familiar parts of bodies that are specific to someone*
221 *you know (e.g., the hands or feet of your parents). The parts of the body you choose*
222 *do not have to belong to the personally familiar people you chose. Please do not*

223 *include explicit body parts. Some examples of body parts specific to a person could*
224 *be hands, feet, legs, arms, whole bodies etc., but not faces.*

225 *For familiar objects, or objects, choose 5 personally familiar objects that are about*
226 *the size of a toaster (e.g., your favorite mug, a coffee maker). These objects should be*
227 *personal items that you know very well and interact with fairly regularly (e.g., your*
228 *personal hairbrush or your soccer ball). You should also be familiar with from multiple*
229 *visual angles or viewpoints.*

230 *For personally familiar places, please list places that you have been to and can*
231 *richly visualize. You should choose places that are personally relevant to you, so*
232 *you should avoid choosing places that you have only been to one time. You should*
233 *not choose famous places where you have never been. You can choose places that*
234 *span your whole life, so you could do your current kitchen, as well as the kitchen*
235 *from your childhood home.*

236 *For famous people, list some celebrities that you do not know personally whose*
237 *faces you can visualize richly. You should be able to imagine their faces and bodies*
238 *moving. For example, if you can imagine Beyonce's face, then she would be a good*
239 *choice. However, if you could only imagine Beyonce's body while she is dancing,*
240 *then you should pick a different celebrity."*

241 During fMRI scanning, participants performed 6 runs of the imagery task. During each run,
242 participants recalled these people, body parts, objects, and places. All stimuli were
243 presented in each run, and trials were pseudo-randomized so that no category could appear
244 on more than 2 consecutive trials.

245 The trial sequence was modelled off our prior work (Steel et al., 2023). On each trial,
246 participants saw the name of a person or place and recalled them in as much detail as
247 possible. The name of the stimulus was displayed for 1 second, followed by a 1 second
248 dynamic mask (mix of ascii characters approximately the same length as the stimulus cue),
249 followed by four circles ('oooo'). Participants were instructed to maintain imagery for as long
250 as the circles remained on the screen (10 s). Trials were separated by a variable ISI (4-8 s).

251 MRI acquisition

252 T1-weighted anatomical scan

253 For registration purposes, a high-resolution T1-weighted magnetization-prepared rapid
254 acquisition gradient echo (MPRAGE) imaging sequence was acquired (TR = 2300 ms,
255 TE = 2.32 ms, inversion time = 933 ms, Flip angle = 8°, FOV = 256 × 256 mm, slices = 255,
256 voxel size = 1 × 1 × 1 mm). T1 images were segmented and surfaces were generated using

257 Freesurfer (Dale et al., 1999; Fischl et al., 2002; Fischl, 2012) (version 6.0) and aligned to the
258 fMRI data using `align_epi_anat.py` and `@SUMA_AlignToExperiment`(Saad and Reynolds,
259 2012).

260 Dataset 1 – Single Echo EPI

261 Single-echo T2*-weighted echo-planar images covering the temporal, parietal, and frontal
262 cortices were acquired using the following parameters: TR=2000 ms, TE=32 ms, GRAPPA=2,
263 Flip angle=75°, FOV=240 x 240 mm, Matrix size=80 x 80, slices=34, voxel size=3 x 3 x 3 mm.
264 To minimize dropout caused by the ear canals, slices were oriented parallel to temporal
265 lobe(Weiskopf et al., 2006). The initial two frames were discarded by the scanner to achieve
266 steady state.

267

268 Dataset 2 & 3 – Multi Echo EPI

269 Multi-echo T2*-weighted sequence. The sequence parameters were: TR=2000 ms,
270 TEs=[14.6, 32.84, 51.08], GRAPPA factor=2, Flip angle=70°, FOV=240 x 192 mm, Matrix
271 size=90 x 72, slices=52, Multi-band factor=2, voxel size=2.7 mm isotropic. The initial two
272 frames of data acquisition were discarded by the scanner to allow the signal to reach steady
273 state.

274 MRI Preprocessing

275 Dataset 1 – Single Echo EPI

276 Data was preprocessed using AFNI (version 20.3.02 'Vespasian')(Cox, 1996). In addition to
277 the frames discarded by the fMRI scanner during acquisition, the initial two frames were
278 discarded to allow T1 signal to achieve steady state. Signal outliers were attenuated
279 (3dDespike). Motion correction was applied, and parameters were stored for use as
280 nuisance regressors (3dVolreg). Data were then iteratively smoothed to achieve a uniform
281 smoothness of 5mm FWHM (3dBlurToFWHM).

282 Dataset 2 & 3 – Multi Echo EPI

283 Multi-echo data processing was implemented based on the multi-echo preprocessing
284 pipeline from `afni_proc.py` in AFNI (version 21.3.10 'Trajan')(Cox, 1996). Signal outliers in the
285 data were attenuated (3dDespike(Jo et al., 2013)). Motion correction was calculated based
286 on the second echo, and these alignment parameters were applied to all runs. The optimal
287 combination of the three echoes was calculated, and the echoes were combined to form a
288 single, optimally weighted time series (T2smap.py). Multi-echo ICA denoising(Kundu et al.,
289 2012; Evans et al., 2015; DuPre et al., 2019, 2021) was then performed (see *Multi-echo ICA*,

290 below). Following denoising, signals were normalized to percent signal change, and data
291 were smoothed with a 3mm Gaussian kernel (3dBlurInMask).

292 *Multi-echo ICA*

293 The data were denoised using multi-echo ICA denoising (tedana.py(Kundu et al., 2012;
294 Evans et al., 2015; DuPre et al., 2019; Steel et al., 2022), version 0.0.12). In brief, PCA was
295 applied, and thermal noise was removed using the Kundu decision tree method.
296 Subsequently, data were decomposed using ICA, and the resulting components were
297 classified as signal and noise based on the known properties of the T2* signal decay of the
298 BOLD signal versus noise. Components classified as noise were discarded, and the
299 remaining components were recombined to construct the optimally combined, denoised
300 timeseries.

301

302 MRI analysis

303 Dataset 1 & 2 GLM and ROI definition

304 *Scene perception area localizer*

305 To define scene perceptual areas, the scene perception localizer was modeled by fitting
306 gamma function of the block duration with a square wave for each condition (Scenes, Faces,
307 and Objects) using 3dDeconvolve. Estimated motion parameters were included as
308 additional regressors of no-interest along with 4th order polynomials. Scene areas were
309 drawn based on a general linear test comparing the coefficients of the GLM during scene
310 versus face blocks. These contrast maps were then transferred to the SUMA standard mesh
311 (std.141) using @SUMA_Make_Spec_FS and @Suma_AlignToExperiment.

312 A vertex-wise significance of $p < 0.001$ along with expected anatomical locations was used to
313 define the pre-constrained regions of interest.

314 *Place memory area localizer*

315 To define place memory areas, the familiar people/places memory data was modeled by
316 fitting a gamma function of the trial duration for trials of each condition (people and places)
317 using 3dDeconvolve. Estimated motion parameters were included as additional regressors
318 of no-interest along with 4th order polynomials. Activation maps were then transferred to the
319 suma standard mesh (std.141) using @SUMA_Make_Spec_FS and
320 @Suma_AlignToExperiment.

321 People and place memory areas were drawn based on a general linear test comparing
322 coefficients of the GLM for people and place memory. A vertex-wise significance threshold
323 of $p < 0.001$ was used to draw the pre-constrained ROIs.

324 Dataset 3 GLM and ROI definition

325 *Dynamic place memory area localizer*

326 To define place memory areas, the familiar people/places memory data was modeled by
327 fitting a gamma function of the trial duration for trials of each condition (famous faces,
328 familiar faces, familiar bodies, familiar objects, familiar places) using 3dDeconvolve (10 s).
329 We included a single regressor to model the cue onset and stimulus mask for all trials (2 s).
330 Estimated motion parameters were included as additional regressors of no-interest along
331 with 4th order polynomials. Activation maps were then transferred to the suma standard
332 mesh (std.141) using @SUMA_Make_Spec_FS and @Suma_AlignToExperiment.

333 People and place memory areas were drawn based on a general linear test comparing
334 coefficients of the GLM for place memory versus all other categories (personally familiar
335 faces, body parts, objects, and famous faces). A vertex-wise significance threshold of
336 $p < 0.001$ was used to draw the pre-constrained ROIs.

337 ROI aggregation across participants

338 Below we detail the procedure for establishing the probabilistic group definition for all
339 regions of interest (scene perception areas: OPA, PPA, MPA; place memory areas: LPMA,
340 VPMA, MPMA).

341 Individual participants exhibit a wide spectrum of activation extent and magnitude during
342 the localizer tasks. To ensure that that these differences did not skew our results and that all
343 individuals contributed equally to the probabilistic parcellation, we constrained the large
344 ROIs drawn from the GLM to the subset of the top 800 most selective surface vertices in each
345 region in their respective task. These vertices had the maximum difference between the
346 category of interest compared to other categories in the task of interest (e.g., in perception,
347 the vertices with the largest difference between scene perception vs face images in Datasets
348 1&2). If the region of interest had fewer than 800 vertices, all vertices were taken.

349 The size of the constrained region (800 vertices) was chosen to balance the size of the
350 regions across subjects, the desire to have the most selective vertices represented, and the
351 desire for contiguity across the vertices. Our prior publications have considered the top 300
352 most selective vertices (Steel et al., 2021, 2023), but this constraint has generally resulted in
353 incontiguous sets of vertices. This led to the adoption of the new, larger set of vertices for
354 parcel definition.

355 We refer to the top 800 most selective vertices as the individualized regions of interest. We
356 aggregated these individualized regions of interest within Datasets 1, 2, and 3 for
357 comparison. We also aggregated across all datasets to form the final probabilistic group
358 parcel definition. We refer to these final probabilistic overlap maps of the individualized
359 regions of interest as “parcels”.

360 Comparison across parcels across datasets

361 We evaluated the success of our parcel definitions for the scene perception and place
362 memory areas by comparing the location of the parcels across Datasets 1-3. For these
363 analyses, we focused on Dataset 1 as the basis for comparison for two reasons. First,
364 Dataset 1 was originally used to establish the place memory areas, and we wanted to
365 confirm that this original definition was consistent. Second, Datasets 2 had the largest
366 number of participants to serve as test cases for the generalization of the established
367 parcels.

368 We performed three different quantifications: 1) overlap between group-level probabilistic
369 maps across datasets, 2) proportion of individual constrained ROIs captured by the group
370 parcel across tasks (i.e., how much did individual participants’ constrained ROIs from
371 Dataset 2 & 3 overlap with the group parcel from Dataset 1), and 3) whether the individual
372 participants’ peak of selectivity was captured by the group parcel across tasks (i.e., did the
373 individual participants’ peak of selectivity from Dataset 2 & 3 fall within the group parcel from
374 Dataset 1). These metrics provide a comprehensive view of the generalization of the parcels
375 in independent data.

376 Shift between scene perception and place memory selectivity

377 In addition to comparing the parcels across datasets, to we also compared the spatial
378 dissociation between the scene perception and place memory areas in all participants. We
379 compared the weighted center-of-mass of the scene perception and place memory areas
380 using the individualized regions of interest from Datasets 1 & 2 (using the methods described
381 in (Steel et al., 2021)). Specifically, we calculated the center of mass of the individualized
382 scene perception and place memory parcels, with the spatial position of each vertex
383 weighted by its selectivity magnitude (i.e., activation for scene versus face perception or
384 place versus face memory).

385 Statistical analysis

386 Statistics were calculated using MATLAB code (Version 2022a, MathWorks). Data
387 distributions were assumed to be normal, but this was not statistically tested. Individual
388 data points are shown. Raleigh’s tests were used to assess the consistency of the direction

389 of the shift from perception to memory. Otherwise, paired t-tests were used where indicated.
390 Alpha level of $p < 0.05$ was used to assess significance, and Bonferroni correction was
391 applied where appropriate.

392 Results

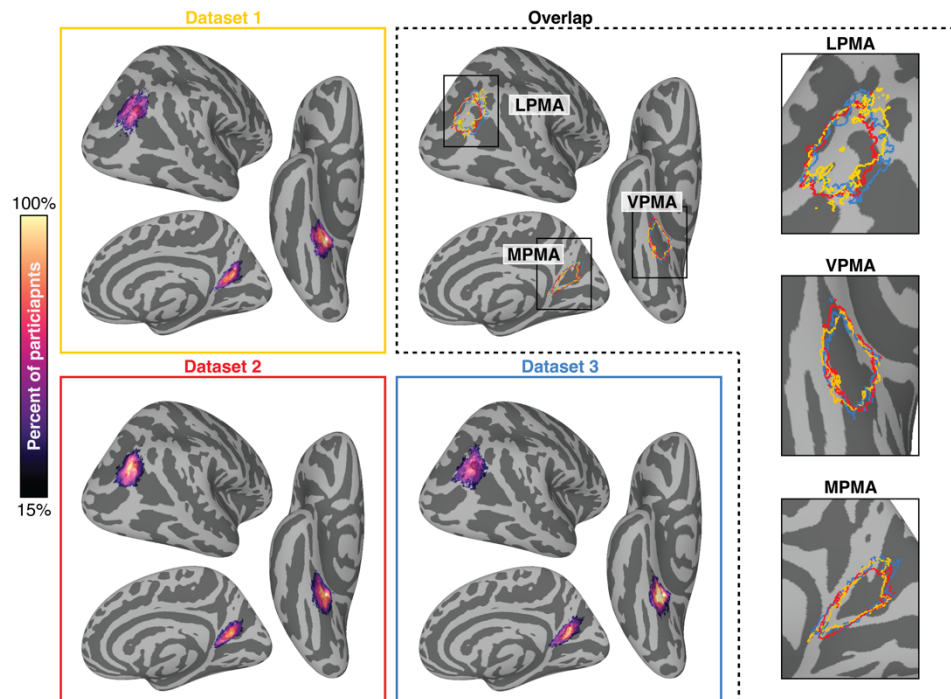
393 The current study had four aims. First, we wanted to establish the localization of the place
394 memory areas across multiple datasets with different data acquisition parameters and
395 experimental design considerations. Second, we wanted to show the consistent
396 topographic extent and location of the place memory areas with respect to their relationship
397 with the scene perception areas at an individual subject level. Third, we wanted to compare
398 the location of the place memory and scene perception areas to other established parcels
399 involved in scene perception at a group level (Julian et al., 2012; Weiner et al., 2018; Rosenke
400 et al., 2021). Finally, we wanted to contextualize the place memory and scene perception
401 areas' locations within the cortical organization more generally, including their anatomical
402 locations, and their location compared to large scale cortical networks and gradients. In
403 addition, we have released a publicly available parcel for the scene perception and place
404 memory areas for general use that can be downloaded from <https://osf.io/xmhn7/>.

405 We defined the place memory areas in individual participants by comparing fMRI activity
406 when participants recalled personally familiar places compared with other categories. In
407 Dataset 1 & 2, we contrasted activation when participants recalled places compared with
408 familiar people's faces. In Dataset 3, we compared activity when participants recalled
409 places versus multiple other categories (places versus faces, objects, bodies, and famous
410 faces). In all Datasets, we defined an initial region of interest for each participant on their
411 lateral, ventral and medial surfaces based on a contrast of $t > 3.3$ ($p = 0.001$, uncorrected).
412 This region of interest was further constrained to the top 800 most selective surface vertices
413 as each participant's "individualized region of interest". These individualized regions of
414 interest served as the basis for comparing across datasets.

415 The place memory areas' location is consistent across datasets

416 We began by comparing the location of the most probable location of the place memory
417 areas across our datasets. Within each dataset (datasets 1-3), we aggregated all
418 participants' individualized regions of interest to derive a probabilistic surface map. In this
419 map, vertices were assigned the probability that they were located within the place memory
420 areas across all individuals in the dataset. We refer to these probabilistic areas as
421 parcels (Rosenke et al., 2021). The probabilistic maps for each parcel and their overlap are
422 shown in Figure 1.

423 We observed a high degree of overlap in place memory parcel's location across the datasets,
424 despite that the datasets considered different data acquisition, processing methods, and
425 task conditions. Qualitatively, the spatial location of the parcels was highly similar, as was
426 the general shape of the cluster. This confirms that the place memory area activation is
427 highly reproducible, which suggests that these regions are a general feature of cortex and do
428 not depend on specific design or acquisition/processing methods. We explore the location
429 of the place memory parcels in greater detail below.



430
431 *Figure 1. The most probable location of the place memory selective activity is consistent across datasets. The most*
432 *probable location of the lateral, ventral, and medial place memory areas (LPMA, VPMA, MPMA) was based on the*
433 *intersection of the top 800 most selective surface vertices for each participant. Probabilistic maps show vertices where*
434 *greater than 15% of participants were represented. The extent of these regions for all datasets are outlined in the upper right*
435 *panel (Dataset 1: Yellow, Dataset 2: Red, Dataset 3, Blue). The boxed portion of the image is enlarged in the insets (right).*

436 Place memory area parcels capture individualized ROIs across datasets

437 Having confirmed that we could reproduce the most probable location of the place memory
438 areas across datasets, we next quantified how well the probabilistic parcels captured the
439 variability of the place memory region of interests' locations in independent participants. We
440 asked two questions: 1) would the probabilistic parcels capture the location of the most-
441 selective vertices from individual-participants from a separate dataset, and 2) how well do
442 the parcels capture the spatial extent of the individualized regions of interest from an
443 independent dataset? Answering these questions will establish whether the most probable

444 location of the parcels is an adequate description of the topography of these functionally
445 defined areas.

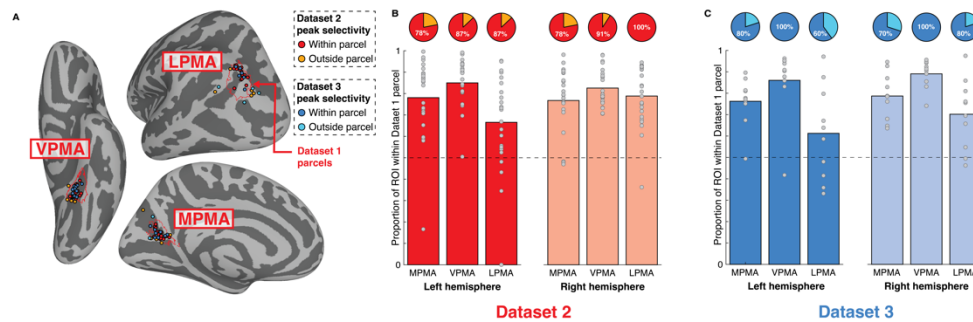
446 For these analyses we used Dataset 1 as the basis for comparison, and we restricted the
447 probabilistic parcels from Dataset 1 with greater than 15% of participants. We used Dataset
448 1 as the basis for comparison for two reasons. First, we used Dataset 1 to establish the
449 location of the place memory areas in our original study (Steel et al., 2021), so this analysis
450 would confirm that our original definition would generalize to new data. Second, Datasets 2
451 and 3 were more appropriate test datasets. Because Dataset 2 had the most participants, it
452 provided the most opportunities to test the generalization of the parcel to new individuals.
453 In addition, because Dataset 3 used a different experimental design, it provided an
454 opportunity to test whether the location of the individualized regions of interest depended
455 on the conditions used to localize these areas. Importantly, three subjects from Dataset 1
456 were also included in Dataset 3; however, because Datasets 1 and 3 used different
457 conditions and came from separate testing sessions, they are still independent. Results
458 were comparable when these participants were removed from the analysis of Dataset 3.

459 Overall, the place memory parcels derived from Dataset 1 generalized to individual
460 participants from Datasets 2 and 3. Across all of the memory areas, the parcels from Dataset
461 1 captured the surface vertex with the greatest selectivity to place memory in the majority of
462 participants in Dataset 2 (Left hemisphere – MPMA: 78%, VPMA: 87%, LPMA: 87%; Right
463 hemisphere – MPMA: 78%, VPMA: 91%, LPMA: 100%) and Dataset 3 (Left hemisphere –
464 MPMA: 80%, VPMA: 100%, LPMA: 60%; Right hemisphere – MPMA: 80%, VPMA: 100%; LPMA:
465 80%) (Figure 2A-B). Qualitatively, most maxima that fell outside of the parcel were very close
466 to parcels' edges (Figure 2A). So, it is possible that these peaks could be captured by the
467 parcel if a more liberal threshold were used.

468 Likewise, the participants' individualized regions of interest from Dataset 2 and 3 (top 800
469 most selective vertices) overlapped substantially with the parcel from Dataset 1 (Figure 2B).
470 We observed significant overlap (> 50%) between individual participants from Dataset 2 and
471 parcel from Dataset 1 in all regions and all hemispheres (Dataset 2: $t_{s(23)} > 3.54$, $p < 0.0018$).
472 For Dataset 3, we observed significant overlap (> 50%) between individual
473 participants in all regions in the right hemisphere ($t_{s(9)} > 3.88$, $p < 0.004$), and in the place
474 memory parcel on the medial and ventral surfaces in the left hemisphere ($t_{s(9)} > 8$, $p < 0.001$);
475 however, the place memory parcel on the lateral surface did not significantly capture
476 greater than 50% of the individualized parcels across participants in Dataset 3 ($t(9) = 1.62$, $p = 0.141$).
477 The results for Dataset 3 were similar when overlapping participants were excluded
478 (Left hemisphere – MPMA: $t(7) = 4.99$, $p = 0.003$; VPMA: $t(7) = 22.90$, $p < 0.001$; LPMA: $t(7) =$
479 1.33 , $p = 0.23$; Right hemisphere – MPMA: $t(7) = 6.30$, $p < 0.001$; VPMA: $t(7) = 31.84$, $p < 0.001$;

480 LPMA: $t(7) = 3.44$, $p = 0.014$). Across both datasets, only one participant (Dataset 2) had zero
481 vertices of their ROI confined to the LPMA parcel in the left hemisphere, which was due to
482 the atypically anterior location of their LPMA ROI compared to other participants.

483 Collectively, these results show that the original place memory parcels established in the
484 subjects from Steel et al., 2021 generalize to new datasets with different data acquisition,
485 processing, and experimental design choices. This suggests that the place memory parcels
486 from one dataset are adequate descriptors of these areas in new datasets, opening the
487 possibility of algorithmic region of interest definition based on these established parcels.



488

489 *Figure 2. Location of place memory areas is consistent across datasets. A. Location of the peaks in place memory area*
490 *parcels (red outline) compared with the individual participant peaks in place memory selective activity from an independent*
491 *set of participants using different fMRI processing and analysis methods (Dataset 2, red) and experimental design (Dataset*
492 *3, blue). Participants with peaks within the parcel are shown in red/blue, peaks outside the parcel are shown in yellow/cyan*
493 *for Datasets 2 and 3, respectively. Only the left hemisphere is shown. These data are summarized as pie charts for both*
494 *hemispheres in panel B and C. B and C. Overlap between the place memory area parcels with individual participant defined*
495 *place memory area ROIs (top 800 memory selective surface vertices) from Dataset 2 (B) and Dataset 3 (C). Pie charts show*
496 *the percentage of participants with peak selectivity contained within the group parcel. Dotted line indicates 50% overlap*
497 *(400 vertices).*

498 Anterior shift for place memory vs. scene perception is reproducible

499 The place memory areas are thought to support mnemonic processes relevant to visual
500 scene analysis, and one key piece of supporting evidence is their proximity to the scene
501 perception areas (Steel et al., 2021). In individual studies, the place memory areas are
502 reported to lie consistently anterior and adjacent to the scene perception areas on their
503 respective cortical surfaces (Steel et al., 2021; Sroková et al., 2022). Next, we tested whether
504 the anterior topographic shift for PMAs relative to SPAs is reproducible across participants
505 in our three datasets. For these analyses, we considered Datasets 1 and 2, which used the
506 same experimental design. The results from Dataset 3 will be reported separately in a future
507 publication.

508 We addressed the relative location of the place memory and scene perception areas in two
509 ways. First, in Datasets 1 and 2, we considered the most probable location of the place
510 memory areas compared to the most probable location of their functionally paired scene
511 perception areas in the same group of participants. Given the similarity of the place memory

512 areas' locations in Datasets 1 and 2 described above, we combined the individualized
513 regions of interest from both Datasets. We then compared topography of the scene
514 perception and place memory area parcels constructed from these combined datasets,
515 including the location of the maximum probability. To evaluate overlap, we thresholded the
516 probabilistic place memory and scene perception parcels to represent at least 33% of
517 participants, a threshold that is consistent with prior publications (Julian et al., 2012; Weiner
518 et al., 2018; Rosenke et al., 2021).

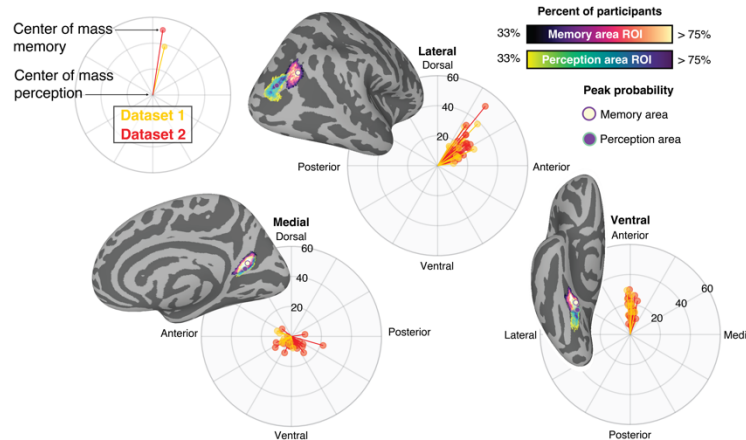
519 We found that the place memory parcel was located anterior to the scene perception area
520 parcel on all cortical surfaces (Figure 3). On the lateral surface, we observed an anterior and
521 dorsal shift of the place memory parcel compared with scene perception, and we saw a
522 relatively small amount of overlap between the memory and perception parcels (Percent of
523 LPMA shared – Left hemisphere = 4.4%; Right hemisphere shared = 8.4%). On the ventral
524 surface, we observed a nearly veridical anterior shift of place memory compared with scene
525 perception and approximately half of the memory parcel was shared with the perception
526 area parcel (Percent of VPMA shared – Left hemisphere = 41.3%; Right hemisphere = 42.9%).
527 On the medial surface, we observed an anterior and dorsal shift in the peak probability
528 between the parcel perception and memory parcels, but these parcels had a high degree of
529 overlap (Percent of MPMA shared – Left hemisphere = 35.6%; Right hemisphere = 61.6%;
530 note that the small amount of LPMA shared is due to the relatively small size of left MPA at
531 an overlap of 33%). These results confirm the spatial dissociation between the place
532 memory and scene perception areas on the lateral surface but suggest a less strong
533 distinction between the memory and perception responses on the medial surface.

534 The prior analysis shows an anterior shift of scene perception and place memory activity at
535 the group level, but it does not capture the consistency of the shift at the individual
536 participant level. We tested the consistency of this shift in a second analysis by comparing
537 the location of the weighted center of mass of each participant's individualized perception
538 and place memory area regions of interests for each cortical surface (Steel et al., 2021). This
539 analysis considers the degree of selectivity for the category of places/scenes versus
540 people/faces during memory and perception, and therefore provides a sensitive measure of
541 activation shifts between conditions in regions with a high degree of intersubject variability.
542 Note that this analysis has been previously published using Dataset 1 with a different ROI
543 definition method (Steel et al., 2021). Here, we replicate that analysis using a new ROI
544 definition (top 800 most selective scene perception and place memory area vertices), and
545 we extend that analysis by considering a new set of participants from Dataset 2. A
546 comparison between scene perception and place memory area activity in Dataset 3 will be
547 presented elsewhere. The results were consistent across hemispheres, so we report the
548 average results across hemispheres.

549 With this approach, we observed a systematic shift of place memory compared with scene
550 perception activation on the lateral and ventral surfaces of the brain. In Datasets 1 and 2, on
551 both lateral and ventral surfaces, the individualized weighted center of mass was
552 significantly anterior to the scene perception area (Dataset 1 – Lateral: $t(13) = 10.22$, $p <$
553 0.001 ; Ventral: $t(13) = 10.11$, $p < 0.001$; Dataset 2 – Lateral: $t(22) = 15.94$, $p < 0.001$; Ventral:
554 $t(22) = 12.17$, $p < 0.001$). On the lateral surface, the angle of this shift was anterior and dorsal,
555 and it highly consistent across individuals (Dataset 1 – mean \pm s.d. shift distance = 20.6 ± 8.4
556 mm., Raleigh’s test: $z = 13.05$, $p < 0.001$; Dataset 2 – mean \pm s.d. shift distance = 21.4 ± 9.6
557 mm, Raleigh’s test: $z = 22.24$, $p < 0.001$). On the ventral surface, the shift was largely anterior,
558 with little medial-lateral variation (Dataset 1 – mean \pm s.d. shift distance = 17.5 ± 7.5 mm,
559 Raleigh’s test: $z = 13.86$, $p < 0.001$; Dataset 2 – mean \pm s.d. shift distance = 16.9 ± 7.8 mm,
560 Raleigh’s test: $z = 22.71$, $p < 0.001$). This replicates the anterior shift previously reported
561 (Steel et al., 2021) using this new individualized ROI definition. Further, this shows that the
562 magnitude of the shift replicates to a larger sample of participants collected using different
563 fMRI acquisition and processing methods.

564 On the medial surface, the displacement of the place memory compared with scene
565 perception activity was less pronounced. We found a significant anterior shift of the place
566 memory compared with scene perception activation on the medial surface in Dataset 1
567 ($t(13) = 2.47$, $p = 0.03$) along a consistent anterior and ventral angle (Mean \pm s.d. shift distance
568 = 6.22 ± 3.0 mm; Raleigh’s test: $z = 8.74$, $p < 0.001$), which replicated our prior result with the
569 new individualized region of interest definition (Steel et al., 2021). However, we did not
570 observe an anterior shift on the medial surface in Dataset 2. While the activity was shifted
571 (Mean shift distance = 7.8 ± 6.2 mm; Raleigh’s test: $z = 7.76$, $p < 0.001$), the shift of memory
572 compared to perception was more ventral ($t(22) = 5.90$, $p < 0.001$) rather than anterior ($t(22)$
573 = 0.79 , $p = 0.43$). Note that the ventral shift of place memory compared with scene
574 perception activity is not consistent with the most probable location of the cluster reported
575 above, where the most probable location of the scene perception area was ventral and
576 posterior to the most probable location of the place memory area. It is likely that the
577 additional information provided by using magnitude of selectivity to weight the center of
578 mass for this analysis led to this discrepancy.

579 Taken together, these results replicate prior work investigating the difference in topography
580 between scene perception and place memory activation in posterior cerebral cortex(Steel
581 et al., 2021). Specifically, the anterior shift for place memory vs. scene perception is most
582 prominent on the lateral surface and ventral surfaces, as compared with the medial surface.
583 This difference between cortical surfaces could belie a difference in the functional
584 distinction between the perception and memory areas across the cortical surfaces (see
585 Discussion).



586

587 *Figure 3. Place memory areas are consistently anterior to scene perception areas. Brain images depict the most probable*
588 *location of the place memory (yellow) and scene perception (purple) areas on the brain's lateral, medial, and ventral*
589 *surfaces based on the overlap of the top 800 most selective vertices for each task across all participants. Rose plots depict*
590 *the shift in the weighted center of mass of place memory compared to scene perception activation in individual*
591 *participants, split between Datasets 1 and 2 (yellow and red, respectively). This individualized analysis revealed a*
592 *consistent shift of place memory compared to scene perception activity on all surfaces (Raleigh's tests: $z_s > 7.6$, $p_s < 0.001$).*
593 *This shift was anterior and dorsal for the lateral surface, anterior on the ventral surface, and ventral on the medial surface.*
594 *Note that rose plots orientation is aligned to the respective brain surface plot. Probability maps for parcels are thresholded*
595 *at 0.33 overlap across participants, consistent with prior work establishing probabilistic locations of functional areas in*
596 *occipito-temporal cortex (Julian et al., 2012; Wang et al., 2015; Weiner et al., 2018; Rosenke et al., 2021).*

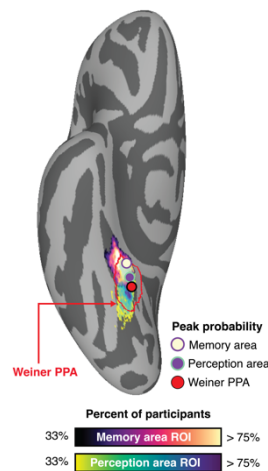
597 Location of the place memory areas compared to established scene 598 perception area definitions

599 The parahippocampal place area (PPA) and occipital place areas (OPA) are critical parts of
600 the scene perception system. These regions can be reliably localized by contrasting brain
601 activity to images of scenes compared to images of other categories like faces, bodies, or
602 objects; however, the precise contrast used varies between research groups. In an effort to
603 standardize the definition of these areas, several groups have published publicly available
604 parcels of the probabilistic locations of PPA and OPA, defined by contrasting activation
605 during place images compared to other categories using different localizer stimuli and scan
606 parameters (Julian et al., 2012; Weiner et al., 2018; Rosenke et al., 2021). How do the place
607 memory and scene perception parcels defined in this study compare with the probabilistic
608 locations of parahippocampal place area and occipital place areas from these independent
609 functional parcels? Specifically, do the place memory areas fall anterior to the probabilistic
610 location of PPA and OPA as defined by these independent datasets? For these analyses, we
611 thresholded our probabilistic parcels to at 33% overlap across participants, consistent with
612 prior work establishing probabilistic locations of functional areas in occipito-temporal
613 cortex (Julian et al., 2012; Wang et al., 2015; Weiner et al., 2018; Rosenke et al., 2021).

614 We compared the location of the place memory and scene perception area parcels to three
615 different publicly available group-defined parahippocampal place areas and two different

616 occipital place areas. First, for parahippocampal place area, we considered a probabilistic
617 definition of this region from Weiner and colleagues (henceforth wPPA) (Weiner et al., 2018).
618 Second, for both parahippocampal place area and occipital place area, we considered an
619 atlas of functionally-defined category selective areas, known as the visf atlas (Rosenke et
620 al., 2021), that includes a scene selective area on the ventral and lateral surfaces (COS-
621 places and TOS-places, respectively). Third, we considered the parahippocampal place area
622 and occipital place area from Julian and colleagues (Julian et al., 2012).

623 In sum, we found that the peak of both our ventral and lateral place memory parcels fell
624 anterior to the peak of every other previously published PPA and OPA/TOS parcel,
625 respectively (Figures 4-6). With reference to the wPPA parcel from Weiner and colleagues
626 (Weiner et al., 2018), we found that the peak of our ventral scene perception parcel
627 corresponded closely to the peak location of the wPPA (Figure 4) (Weiner et al., 2018). While
628 our scene perception parcel extended posteriorly beyond the wPPA, the maximum
629 probability was well aligned between these areas. Importantly, the place memory parcel
630 extended anteriorly beyond the wPPA, and the peak in probability of the place memory
631 parcel was anterior to peak in probability from the wPPA. This suggests that the scene
632 perception parcels we defined are well aligned with this definition of the parahippocampal
633 place area (as previously shown) (Steel et al., 2021).



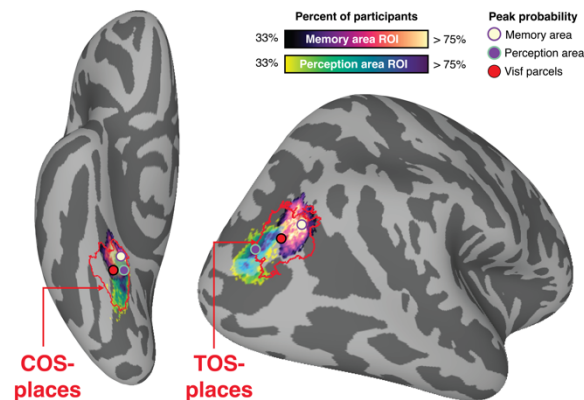
634

635 *Figure 4. Location of most probable location of the place memory and scene perception parcels compared*
636 *parahippocampal place area defined by Weiner and colleagues (red outline) (Weiner et al., 2018). Place memory area*
637 *parcels combine the most probable locations of participants in Datasets 1 and 2 (33% of participants). Probable location*
638 *data is reproduced from Figure 3.*

639 Second, we considered the visf atlas (Rosenke et al., 2021), which contained a ventral and
640 lateral scene selective area analogous to the parahippocampal place area and occipital
641 place area (referred to as COS-places and TOS-places); notably COS-places from has a
642 significantly greater anterior extent compared to the wPPA (Rosenke et al., 2021). We found

643 that COS-places extended anteriorly beyond our ventral scene perception area parcel
644 (Figure 5). Consequently, we observed more overlap between the place memory area parcel
645 with COS-places. TOS-places also had a greater anterior extent than the lateral scene
646 perception area parcel, and therefore also overlapped more with the place memory parcel.
647 We found that the TOS-places region of interest overlapped with the peak of probability of
648 both the scene perception and place memory parcels on the lateral surface. Importantly, the
649 place memory parcels were still anteriorly shifted compared to COS-places and TOS-
650 places, which supports our conclusion that the place memory parcels are distinct from
651 functionally localized visual areas.

652

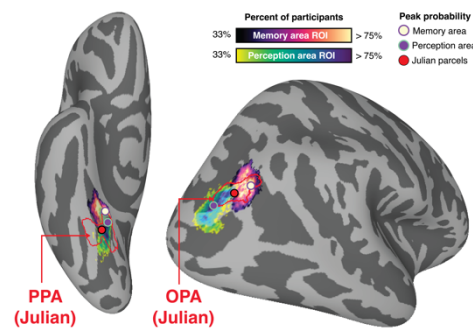


653

654 *Figure 5. Location of most probable location of the place memory and scene perception parcels compared to COS-places*
655 *and TOS-places defined in the visf atlas (red outline) (Rosenke et al., 2021). Place memory area parcels combine the most*
656 *probable locations of participants in Datasets 1 and 2 (33% of participants). Probable location data is reproduced from*
657 *Figure 3.*

658 Third, we considered the parcels from Julian and colleagues (Julian et al., 2012), which
659 contained parahippocampal place area and occipital place area atlas regions of interest
660 (henceforth jPPA and jOPA, respectively). Interestingly, we found mixed topographic
661 relationship between our scene perception and place memory area parcels and the Julian
662 regions of interest (Figure 6). Although we found that the jPPA captured the maximum
663 probability of our ventral scene perception parcel, our parcel had a larger anterior and
664 posterior extent, and we observed relatively little overlap between the jPPA and our place
665 memory parcel. On the lateral surface, the jOPA was shifted anteriorly compared to our
666 lateral scene perception parcel. Like TOS-places from the visf atlas, the jOPA overlapped
667 with the maximum probability of both our scene perception and place memory parcel.
668 However, the lateral place memory parcel was distinct from the jOPA: the lateral place
669 memory parcel had a greater dorsal-ventral extent compared to the jOPA, and the lateral
670 place memory parcel was shifted anteriorly compared with the jOPA. Thus, the Julian scene

671 perception area regions of interest were qualitatively different in their topographic extent
672 from the parcels defined from our data.



673
674 *Figure 6. Location of most probable location of the place memory and scene perception parcels compared to*
675 *parahippocampal place area (PPA) and occipital place area (OPA) regions of interest defined by Julian and colleagues (red*
676 *outline) (Julian et al., 2012). Place memory area parcels combine the most probable locations of participants in Datasets 1*
677 *and 2 (33% of participants). Probable location data is reproduced from Figure 3.*

678 Place memory areas are at an inflection point between unimodal and 679 transmodal cortex

680 The previous results demonstrated the robust localization of place memory selective areas
681 showed the consistent topographic distinction (anterior shift) between the place memory
682 activity compared with scene perception activity. Next, we investigated the location of the
683 place memory and scene perception parcels compared with other proposed anatomical and
684 functional landmarks of cerebral cortex. Comparing the locations to established landmarks
685 will provide a more comprehensive understanding the place memory area's position cortex
686 more generally.

687 Glasser atlas

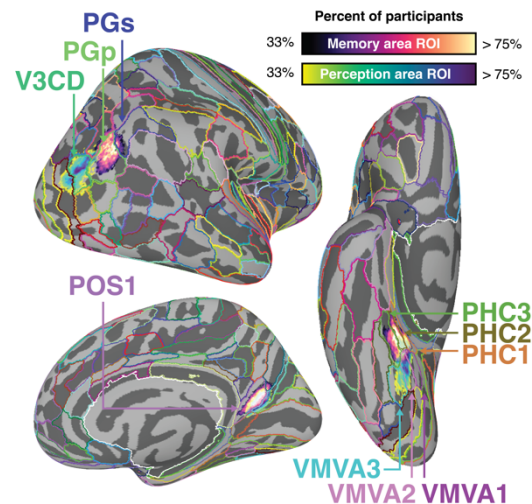
688 First, to better understand the place memory and scene perception location relative to
689 known anatomical landmarks, we compared these parcels to the multimodal atlas from
690 Glasser and colleagues (Glasser et al., 2016). We used the probability maps for the place
691 memory and scene perception areas combined from Datasets 1 and 2 thresholded to
692 consider only vertices with greater than 33% of participants represented.

693 The place memory and scene perception areas were largely centered on different known
694 anatomical landmarks from the Glasser parcellation (Figure 7). On the lateral surface, the
695 place memory parcel was situated over PGp and only minimally overlapped with other areas
696 posterior to PGp. The place memory parcel did extend anteriorly and dorsally into PGs and
697 intraparietal area 0 and 1. Overall the place memory parcel location may be qualitatively
698 similar location to the tertiary sulcus slocs-v, based on visual comparison with published
699 maps (Willbrand et al., 2024). On the other hand, the lateral scene perception parcel was

700 situated more posteriorly, falling largely within area V3CD and posteriorly into the fourth
701 visual area. The portion of the scene perception parcel shared with the place memory parcel
702 did extend anteriorly into PGp and interparietal area 0, ventrally into LO1, dorsally into V3B.

703 On the ventral surface, the place memory parcel began at the anterior portion of the
704 ventromedial visual areas 1-3 and covered the full extent of parahippocampal areas 1-3. The
705 medial portion of the place memory parcel crossed minimally into presubiculum. The
706 anterior portion did not overlap with entorhinal or perirhinal cortex, and the posterior extent
707 of the place memory parcel only minimally overlapped with the ventromedial visual areas 1-
708 3. In contrast, the ventral scene perception parcel was situated within the ventromedial
709 visual areas 1-3, and centered on ventromedial visual area 2. The scene perception parcel
710 did extend anteriorly into the middle of parahippocampal areas 1-3.

711 On the medial surface, both the medial place memory and scene perception parcels
712 covered the full extent of parieto-occipital area sulcus area 1 and terminated prior to
713 retrosplenial complex. Both parcels overlapped with the transitional visual area and parieto-
714 occipital sulcus area 2. Neither the place memory or scene perception parcel extended
715 anterior-dorsally into area 23 A/B or area 7M.



716

717 *Figure 7. Location of most probable location of the place memory and scene perception parcels compared to the*
718 *anatomical regions from the Glasser MPM atlas (Glasser et al., 2016) (Glasser 2016). On the lateral and ventral surfaces,*
719 *the peak probability of the place memory area was centered in a region anterior to the scene perception area. On the lateral*
720 *surface, the maximal probability was at the boundary between PGp and PGs, while the scene perception area peak was in*
721 *V3CD. On the ventral surface, the place memory area parcel was centered on PHC1-3, while the scene perception area was*
722 *located primarily within the VMVA1-3. On the medial surface, both the scene perception and place memory area were*
723 *largely confined within POS1. Place memory area parcels combine the most probable locations of participants in Datasets*
724 *1 and 2 (33% of participants). Probable location data is reproduced from Figure 3.*

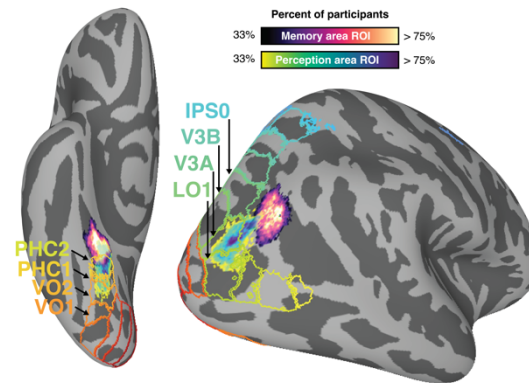
725 Retinotopic maps (Wang atlas)

726 Retinotopic maps, topographic recapitulations of the retina based on voxels' preferential
727 responses to stimulation of portions of the visual field, are a hallmark of visual cortical
728 organization. Although the visual field preferences are shared between retinotopic maps,
729 many of the retinotopic maps have dissociable roles in visual processing (e.g., the
730 independent processing of orientation and shape in LO1 versus LO2 (Silson et al., 2013)).
731 Understanding the location of the scene perception and place memory parcels relative to
732 these retinotopic maps will help understand these areas' locations compared to these well-
733 characterized sub-regions of classically visually responsive cortex. To this end, we
734 compared the most probable location of these parcels with the most probable location of
735 the retinotopic maps using the atlas from (Wang et al., 2015).

736 We found that the scene perception parcel largely fell within the retinotopic maps, while the
737 place memory parcel was generally anterior to these maps, consistent with their respective
738 roles in perception and memory (Figure 8). On the ventral surface, the peak of scene
739 perception area probability fell within map PHC2, and the parcel extended posteriorly as far
740 as map VO1. In contrast, the peak probability of the ventral place memory area parcel was
741 anterior to map PHC2. The place memory area parcel did extend posteriorly into the PHC2
742 parcel, but much of the parcel was anterior to the map.

743 On the lateral surface, the location of the perception and memory parcels followed a similar
744 pattern to the ventral surface. Most of the scene perception parcel fell within the retinotopic
745 maps LO1, V3A, and V3B, and the peak of scene perception parcel probability fell within V3A.
746 On the other hand, the place memory parcel was anterior to these maps, nestled within the
747 space not considered classically visually responsive between maps LO2, LO1, V3A, V3B,
748 IPS0, and IPS1.

749 Taken together, these results show that the place memory parcels are largely anterior to
750 classic retinotopic maps. This is generally consistent with the assumed dissociation with
751 their functional roles. Notably, recent work has shown that the place memory areas have
752 nontraditional visual responses, including systematic negative BOLD responses to
753 stimulation of positions on the retina (negative retinotopic coding) (Angeli et al., 2024; Steel
754 et al., 2024b, 2024a), consistent with much of the default mode network of the brain (Szinte
755 and Knapen, 2020; Christiaan Klink et al., 2021). The difference in visual coding between the
756 scene perception and place memory areas adds to the evidence for their distinct roles in
757 cognition.



758

759 *Figure 8. The place memory areas fall outside of the retinotopic maps, while the scene perception areas fall largely within*
760 *these maps. Retinotopic maps were defined using a maximum probability projection from a standard atlas (Wang et al.,*
761 *2015). Place memory area parcels combine the most probable locations of participants in Datasets 1 and 2 (33% of*
762 *participants). Probable location data is reproduced from Figure 3.*

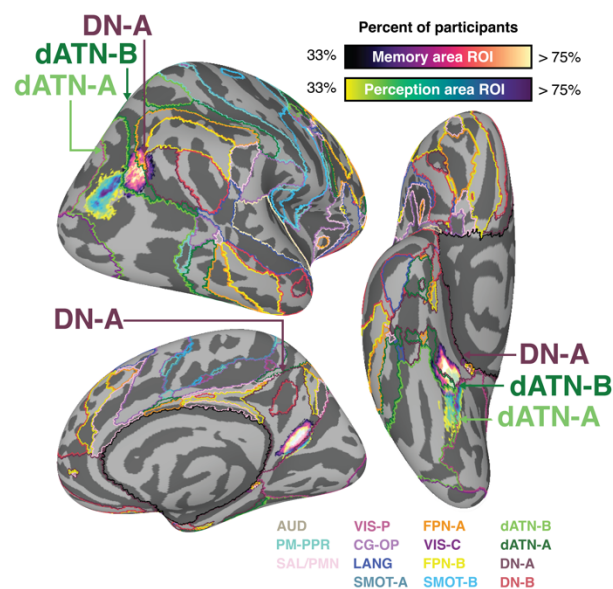
763 Large-scale cortical networks (Yeo HCP 15)

764 Within human cognitive neuroscience, there is a growing consensus that the coordinated
765 activity across large-scale distributed networks of brain areas underpins cognitive
766 processes like external attention, episodic projection, social processing, and language
767 comprehension and production (Fox et al., 2005; Buckner et al., 2011; Power et al., 2011;
768 Braga and Buckner, 2017; DiNicola et al., 2020; DiNicola and Buckner, 2021; Du et al., 2024;
769 Steel et al., 2024a). Establishing where the place memory and scene perception parcels are
770 located compared to these distributed networks will help contextualize how these regions
771 contribute to the brain's large-scale activity. Importantly, these distributed cortical networks
772 can be defined within individual participants with sufficient resting-state fMRI
773 data (Laumann et al., 2015; Braga and Buckner, 2017; Gordon et al., 2017; Gratton et al.,
774 2018; DiNicola and Buckner, 2021; Du et al., 2024). However, it is also common to use
775 established templates of these networks for group analysis (Buckner et al., 2011) or as priors
776 for individualized network definition (Kong et al., 2021; Du et al., 2024). So, here we
777 compared the most probable location of the place memory and scene perception parcels to
778 a commonly used template from Yeo and colleagues (Buckner et al., 2011).

779 Overall, the scene perception and place memory parcels were associated with networks
780 involved in external and internally oriented attention, respectively (Raichle et al., 2001; Fox
781 et al., 2005, 2006; Steel et al., 2024a) (Figure 9). Specifically, the peak probability of the
782 scene perception area parcels on the lateral and ventral surfaces fell within the dorsal
783 attention network A, a network typically associated with externally oriented attention due to
784 its activation during attentionally-demanding visual tasks (e.g., visual search) (Fox et al.,
785 2005, 2006). On the other hand, the place memory parcels tended to fall at the boundary
786 between the dorsal attention network B and the default network A, generally associated with

787 high-level visual processing and episodic projection and scene construction tasks,
788 respectively (Braga and Buckner, 2017; Dixon et al., 2017; DiNicola et al., 2020). On the
789 medial surface, both place memory and scene perception parcels were at the posterior-
790 ventral edge of the large default network A cluster in posterior parietal cortex.

791 These data are consistent with the role of the scene perception area in high-level visual
792 analysis. Moreover, they suggest that the place memory parcels may be a transitional zone
793 between external and internally oriented neural systems that are not well captured by the
794 canonical networks. However, this should be interpreted with caution, as the topography of
795 these networks is more accurate when defined in individual participants (Gordon et al.,
796 2017).



797

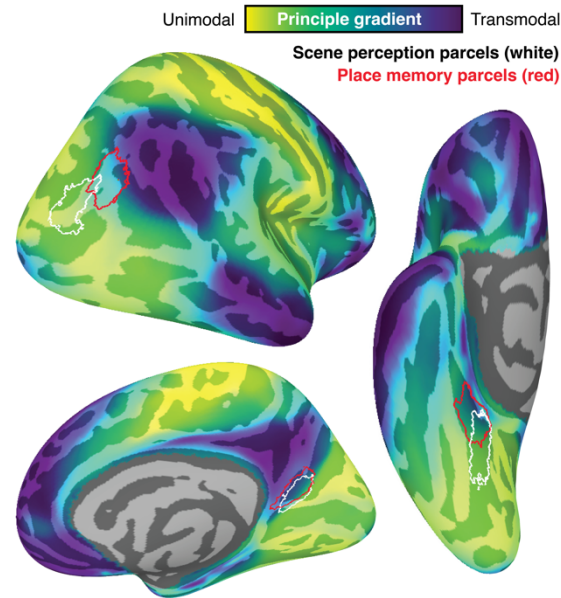
798 *Figure 9. Location of most probable location of the place memory and scene perception parcels compared to the large-*
799 *scale distributed cortical networks defined by Yeo and colleagues (colored outlines) (Buckner et al., 2011). On the lateral*
800 *and ventral surfaces, the scene perception areas fell largely within sensory grounded cortical networks, specifically dATN-*
801 *A. On the other hand, the place memory area parcels fell within networks associated with more abstract, mnemonic*
802 *processing, including the DN-A and dATN-B. On the medial surface, both the scene perception and place memory area*
803 *parcels fell within DN-A. Place memory area parcels combine the most probable locations of participants in Datasets 1 and*
804 *2 (33% of participants). Probable location data is reproduced from Figure 3.*

805 Principle gradient (Margulies et al., 2016)

806 Beyond discrete networks, cortical organization can be characterized by continuous
807 gradients that transition from unimodal sensory/motor areas to transmodal association
808 areas. These gradients are thought to reflect increasingly abstract and integrated
809 information processing (Margulies et al., 2016; Huntenburg et al., 2018; Murphy et al., 2018,
810 2019). Given that place memory areas appear to bridge perceptual and mnemonic
811 processes, understanding their position along this gradient could provide insight into their
812 functional role. Using the principal gradient framework established by Margulies et al., we
813 examined where scene perception and place memory areas fall along this unimodal-to-
814 transmodal axis (Margulies et al., 2016). We hypothesized that scene perception areas,
815 which process immediate visual input, would occupy a relatively unimodal position. In
816 contrast, we predicted place memory areas would fall further along the gradient toward
817 transmodal cortex, reflecting their role in integrating visual and mnemonic information.

818 For this analysis, we compared the location of the place memory and scene perception
819 parcels with the first principal gradient published by Margulies and colleagues (Margulies et
820 al., 2016). We restricted these parcels to surface vertices with greater than 33% of
821 participants.

822 We found that the place memory and scene perception parcels were in distinct portions of
823 the unimodal-to-transmodal axis (Figure 10). Consistent with our hypothesis, the scene
824 perception parcels fell largely within unimodal cortex. Intriguingly, on all cortical surfaces,
825 the place memory parcels fell at the inflection point between unimodal and transmodal
826 cortex, and the parcels spanned the dominantly unimodal to more dominantly transmodal
827 cortical territory. This is further support for the distinct roles of the scene perception and
828 place memory areas, and specifically that the place memory areas may constitute a unique
829 transition zone between sensory and abstract representations.

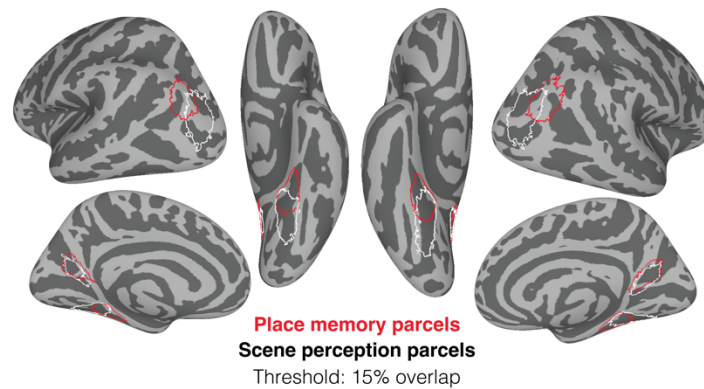


830

831 *Figure 10. The scene perception and place memory areas are located at different points along the unimodal-to-transmodal*
832 *principal gradient. On the lateral and ventral surfaces, the scene perception parcels are largely confined to unimodal*
833 *cortical territory. In contrast, the place memory parcels fall at the inflection point between unimodal and transmodal*
834 *cortical territory. Principal gradient data are taken from Margulies et al., 2016(Margulies et al., 2016). Place memory and*
835 *scene perception parcels were binarized probability maps containing at least 33% of participant's individualized perception*
836 *or memory area regions of interest.*

837 Place memory and scene perception parcel availability and access

838 Taken together, these data support the distinction between scene perception and place
839 memory related activity on the lateral and ventral surfaces. Figure 11 shows a binarized mask
840 of the probabilistic definition of the scene perception and place memory parcels for both
841 hemispheres reported here (thresholded at 15% participants), which are available for
842 download here: <https://osf.io/xmhn7/>. The 15% threshold was chosen because of the
843 relative success in capturing the individual local maxima across independent datasets
844 (Figure 2, above). Parcels are available as volume (nifti) and surface files (SUMA's NIML
845 standard mesh 141 density (Argall et al., 2006; Saad and Reynolds, 2012) and Gifti formatted
846 for the fsaverage template (Fischl, 2012)). We have released a probabilistic definition of
847 these parcels for users who wish to set their own parcel probability criteria. Finally, we have
848 released stimulus presentation code and instructions to run the place memory localizer
849 used in this study.



850

851 *Figure 11. Place memory and scene perception area binarized parcels. Vertices within the parcel were present in greater*
852 *than 15% of participant's individualized perception or memory area regions of interest.*

853 Discussion

854 Here, we characterized the anatomical locations of the place memory areas, a set of brain
855 areas that respond more when participants recall personally familiar places compared with
856 other types of stimuli (Steel et al., 2021), across a relatively large group of participants
857 spanning three different studies. We made three central observations. First, the place
858 memory areas' locations are consistent across participants and different fMRI acquisition
859 parameters, localizer tasks, and statistical contrasts. Second, within a participant, the place
860 memory areas lie systematically anterior to the scene perception areas on the lateral and
861 ventral surfaces. Third, at the group-level, compared with the scene perception areas, the
862 place memory areas are in regions associated with memory processes. Specifically, the
863 place memory areas are immediately anterior to the retinotopic maps and previous
864 published definitions of the scene perception areas (Julian et al., 2012; Wang et al., 2015;
865 Weiner et al., 2018; Rosenke et al., 2021), at the boundary between Dorsal Attention Network
866 B and the Default Network B (Buckner et al., 2011), and span the transition between
867 unimodal and transmodal cortex (Margulies et al., 2016). These group analyses support the
868 hypothesis that the place memory areas serve as a bridge between perceptual and
869 mnemonic processes in cortex (Steel et al., 2021, 2023, 2024b, 2024a; Angeli et al., 2024).

870 Place memory areas are consistently anterior to scene perception areas 871 on the lateral and ventral surfaces

872 A striking feature of the place memory and scene perception areas is their topographic
873 arrangement in cortex. Our initial description revealed that the place memory areas were
874 located immediately anterior and adjacent to the scene perception areas within individual
875 subjects (Steel et al., 2021), which was subsequently replicated by our group and others

876 (Srokova et al., 2022; Steel et al., 2023, 2024b). The precise arrangement between
877 perception and mnemonic areas varies by cortical surface: the trajectory between from
878 scene perception to place memory area is dorsal and anterior on the lateral surface, anterior
879 and ventral on the medial surface, and anterior on the ventral surface. In addition, earlier
880 studies found a larger anterior shift for the lateral and ventral place memory areas vs. their
881 corresponding scene perception areas, as compared with the medial areas (Steel et al.,
882 2021; Srokova et al., 2022). Our findings here replicate these prior findings, with remarkable
883 consistency between the Datasets. The reproducibility of this shift across participants and
884 paradigms suggests that a neuroanatomical linking mechanism (e.g., structural
885 connectivity) may underpin their co-localization.

886 Unlike the lateral and ventral surfaces, the medial place memory and scene perception
887 areas were highly overlapping, and the shift of memory versus perception was smaller and
888 less consistent. The findings from Dataset 1 replicate the original observation of an anterior
889 (and ventral) shift for the center of mass of memory compared with perception on the medial
890 surface (Steel et al., 2021). However, we found no anterior shift in Dataset 2. Instead, we
891 observed a ventral shift of memory compared with perception in Dataset 2, but this shift was
892 small compared with the shift on the other cortical surfaces (approximately 7mm shift on
893 the medial versus 18 or 21 mm shift on the ventral and lateral surfaces). In both Datasets,
894 we observed a considerably more overlap between the perception and memory areas on the
895 medial surface compared with the lateral and ventral surfaces. As noted in the initial studies
896 of these areas, these differences suggest that the relationship between memory and
897 perception on the medial surface may be categorically different than the lateral and ventral
898 surfaces(Steel et al., 2021, 2023).

899 What does the co-localization memory and perceptual activity for scenes on the medial
900 surface imply about the medial scene regions' functions? Prior work suggests that the
901 medial scene perception area may not be involved in visual analysis, per se, like image
902 processing related to structure identification (i.e., "this is a tower") or path detection,
903 associated with the ventral and lateral surfaces, respectively (Marchette et al., 2015; Julian
904 et al., 2016; Kamps et al., 2016; Persichetti and Dilks, 2016, 2019; Bonner and Epstein, 2017;
905 Epstein and Baker, 2019; Henriksson et al., 2019; Lescroart and Gallant, 2019; Dilks et al.,
906 2022). Instead, the medial scene perception area may be involved with more abstract
907 processes related to joint visuo-mnemonic representation(Epstein et al., 2007; Park et al.,
908 2007; Baumann and Mattingley, 2010; Vass and Epstein, 2013; Marchette et al., 2014;
909 Robertson et al., 2016; Silson et al., 2018; Berens et al., 2021). Prior work has established a
910 role for the posterior medial parietal cortex near the parietooccipital sulcus, often referred
911 to as retrosplenial complex, in scene memory and navigation (Maguire et al., 1998; Epstein
912 et al., 2007; Auger et al., 2015; Chrastil et al., 2018; Steel et al., 2019, 2021; Foster et al.,

913 2023). This area is more active when viewing images of familiar scenes compared with
914 unknown scenes (Epstein et al., 2007; Steel et al., 2021). In addition, when viewing familiar
915 scenes, the posterior medial parietal cortex represents allocentric position of that scene in
916 the environment (Baumann and Mattingley, 2010; Vass and Epstein, 2013; Marchette et al.,
917 2014; Nau et al., 2020). In addition, if the spatial relationship between scenes is known (e.g.,
918 they appear on opposite sides of a street), the medial place area represents the spatial
919 relationship between these viewpoints within a larger panoramic environment (Robertson et
920 al., 2016; Berens et al., 2021). Collectively, these functions rely on mnemonic information
921 associated with familiarity.

922 Taken together, these results show a qualitative distinction between the importance of
923 memory in the (nominally) scene perception area on the medial surface. This portion of
924 cortex also activates during mental imagery of scenes, when recalling past events, and
925 imagining future events (Gilmore et al., 2015, 2016; Vass and Epstein, 2017; Silson et al.,
926 2018, 2019; Barry et al., 2019; DiNicola et al., 2020). In our data, we observe little distinction
927 between perceptual and mnemonic activity on the medial surface, with visual scene
928 perception tasks activating just a small portion of this larger, memory responsive region.
929 Therefore, we suggest that future work distinguishing between mnemonic and perceptual
930 processing in scenes might jointly consider this scene perception area (MPA/RSC) and its
931 mnemonic counterpart MPMA as single memory area, akin to LPMA and VPMA, and separate
932 from scene perception areas on the ventral and lateral surface (PPA and OPA). Notably, at a
933 finer scale, the anterior and posterior banks of the parietooccipital sulcus may be
934 differentially involved in memory and perception (Silson et al., 2016, 2018), and it is possible
935 that these fine-grained distinctions have been blurred at 3T resolution used in this study.
936 Future work using high- or layer- resolution fMRI may more clearly characterize the visual
937 selectivity and processes in the medial scene perception and place memory areas.

938 Place memory areas span the transition from unimodal to transmodal 939 cortex

940 Our analyses revealed the place memory areas' intriguing position at the intersection of
941 perceptual and mnemonic cortical systems. Rather than simply activating either sensory
942 regions or memory-related networks like the default network (DiNicola et al., 2020; Du et al.,
943 2024), these areas emerge at their intersection, suggesting they may serve as a functional
944 bridge between these systems. This pattern was particularly clear in our large-scale network
945 analyses, where both VPMA and LPMA peaked at the boundary between the dorsal attention
946 network B and the default network A, which are associated with external and internally
947 oriented attention respectively (Fox et al., 2005; Dixon et al., 2017; Murphy et al., 2018, 2019).
948 Likewise, the place memory areas fell at the inflection point between unimodal and

949 transmodal cortical territory (Margulies et al., 2016). This position allows these areas serve
950 as a topographic link between perceptual and mnemonic systems to facilitate their
951 interaction during complex behaviors like navigation that require continuous interplay
952 between perception and memory.

953 The transitional nature of the place memory areas was further supported by their
954 relationship to know retinotopic maps (Wandell et al., 2007; Wang et al., 2015). Our group
955 analysis underscored that the memory areas fell at the anterior edge of the known
956 retinotopic maps, implying that they are interfacing with retinotopic information. However,
957 these areas may not have a map-like topographic layout typically associated with visually
958 responsive areas. Instead, our previous work has shown that these regions have a significant
959 proportion of negative retinotopic voxels (Steel et al., 2024b). Recent work has shown that
960 this bivalent (negative vs. positive) retinotopic code underpins voxel-scale interactions
961 across place memory and scene perception areas (Steel et al., 2024b), and broader
962 perceptual-mnemonic interactions in the brain, including interactions between the default
963 network and dorsal attention network (Steel et al., 2024a) and between the hippocampus
964 and cortex (Angeli et al., 2024). The place memory areas' position at the edge retinotopic
965 cortex and their mixed response properties suggests that they may organize the retinotopic
966 information transfer across cortical systems. However, because these results consider
967 group-aligned data, future work with high-resolution fMRI with dense sampling individual
968 participants will be critical to investigate these areas' possible role in bridging perceptual
969 and mnemonic representation and whether these transitional areas are a general motif of
970 cortical organization.

971 An important contribution of this work is characterizing place memory areas within
972 previously established anatomical atlases and functional frameworks. For example, one
973 prominent framework of perceptual-mnemonic systems, the PMAT framework (Ranganath
974 and Ritchey, 2012; Ritchey et al., 2015; Reagh and Ranganath, 2018, 2023; Barnett et al.,
975 2021), posits a “medial temporal network” (MTN), a set of brain areas including the
976 parahippocampal cortex and precuneus, bridges visual areas to the DMN and the
977 hippocampus ((Barnett et al., 2021), see also (Andrews-Hanna et al., 2014; Gilmore et al.,
978 2016)). Additionally, within the DMN, two subsystems – the posterior medial networks (PMN)
979 and the anterior temporal network (ANT) – are thought to represent place (i.e., location,
980 situation) and item information (i.e., objects and people), respectively (Ranganath and
981 Ritchey, 2012; Ritchey et al., 2015; Reagh and Ranganath, 2018; Cooper and Ritchey, 2019;
982 Ritchey and Cooper, 2020). Consistent with the PMAT framework, our group analysis shows
983 that the place memory areas overlap with the MTN described by Barnett and colleagues
984 based on their associated Glasser parcels (Glasser et al., 2016). Specifically, both the place
985 memory areas and the MTN are associated with the parahippocampal areas 1-3 and the PGp

986 on the ventral and lateral surface, respectively. Showing this correspondence deepens our
987 understanding of the place memory areas broader functional profile, implicating them more
988 directly in autobiographical memory, scene construction, and navigation (Ranganath and
989 Ritchey, 2012; Cooper and Ritchey, 2019; Ritchey and Cooper, 2020; Barnett et al., 2021). It
990 also suggests that the place memory areas' visual properties and functions during memory-
991 guided visual tasks, including their retinotopic coding (Steel et al., 2024b) their role in
992 representing visuospatial context (Steel et al., 2023), could be integrated within the PMAT
993 framework. More broadly, this approach of situating brain areas within multiple reference
994 frameworks helps synthesize findings across different theoretical perspectives and
995 methodological approaches.

996 Place memory areas can be localized across different datasets and 997 protocols

998 Our results show that the place memory areas are localizable in a larger group of
999 participants and when considering a broader set of categories in memory (as is common in
1000 studies of perception, e.g., (Stigliani et al., 2015; Weiner et al., 2018; Gomez et al., 2019;
1001 Allen et al., 2021; Rosenke et al., 2021)). Importantly, we found these areas in all 44
1002 participants we scanned, and the location of the place memory areas was consistent
1003 between groups using simple two-category contrast (familiar places versus familiar faces
1004 memory recall) or multiple categories (familiar places versus familiar faces, objects, bodies,
1005 famous faces). Taken together, these results show that the place memory areas a robust
1006 feature of human functional brain organization.

1007 Interestingly, although the place memory parcels were significantly more anterior than all
1008 previous scene perception area parcels, including the wPPA (Weiner et al., 2018), CoS-
1009 places and TOS-places region (visf atlas)(Rosenke et al., 2021), and jPPA and jOPA (Julian
1010 parcels) (Julian et al., 2012), our lateral scene perception parcel was generally more
1011 posterior than previous scene perception parcels (TOS-places and jOPA). Several
1012 methodological differences may explain this partial discrepancy. First, these prior parcels
1013 were defined by contrasting activation when participants viewed scenes versus multiple
1014 other visual categories, while we used a more targeted scenes versus faces contrast to
1015 match our place memory localizer (places versus people recall). Second, task demands
1016 differed across studies - we used passive viewing whereas the data used to define the visf
1017 atlas employed an oddball task (Rosenke et al., 2021); Julian et al. did not report task
1018 details(Julian et al., 2012). These differences in stimuli and attention demands could
1019 contribute to the observed variability in parcel location. Taken together, our results reinforce
1020 the distinction between scene perception and place memory areas on both lateral and

1021 ventral surfaces, and our publicly available probabilistic parcels complement existing
1022 resources by providing bilateral, probabilistic ROIs that capture this distinction.

1023 Conclusion

1024 To summarize, understanding the neural systems that subserve perceptual-mnemonic
1025 interactions is a critical question for neuroscience. Here, we describe the anatomical
1026 location of the place memory areas (PMAs) on the brain's lateral, ventral and medial surface,
1027 which are well poised to facilitate perceptual-mnemonic interactions for scenes. Further
1028 study of these brain areas could yield critical insights into neural processes underpinning
1029 spatial cognition and other functions that require the dynamic interplay between perception
1030 and memory. To support this, we have released the probabilistic maps and parcels defined
1031 in the large group of participants for public use (<https://osf.io/xmhn7/>).

1032

1033 References

- 1034 Allen EJ, St-Yves G, Wu Y, Breedlove JL, Prince JS, Dowdle LT, Nau M, Caron B, Pestilli F,
1035 Charest I, Hutchinson JB, Naselaris T, Kay K (2021) A massive 7T fMRI dataset to bridge
1036 cognitive neuroscience and artificial intelligence. *Nature Neuroscience* 2021 25:1
1037 25:116–126 Available at: <https://www.nature.com/articles/s41593-021-00962-x>
1038 [Accessed April 16, 2024].
- 1039 Andrews-Hanna JR, Smallwood J, Spreng RN (2014) The default network and self-generated
1040 thought: Component processes, dynamic control, and clinical relevance. *Ann N Y Acad
1041 Sci* 1316:29–52.
- 1042 Angeli PA, Steel A, Silson EH, Robertson CE (2024) Positive and Negative Retinotopic Codes
1043 in the Human Hippocampus. *bioRxiv:2024.09.27.615397* Available at:
1044 <http://biorxiv.org/content/early/2024/10/05/2024.09.27.615397.abstract>.
- 1045 Argall BD, Saad ZS, Beauchamp MS (2006) Simplified intersubject averaging on the cortical
1046 surface using SUMA. *Hum Brain Mapp* 27:14–27 Available at:
1047 <https://pubmed.ncbi.nlm.nih.gov/16035046/> [Accessed June 28, 2022].
- 1048 Auger SD, Zeidman P, Maguire EA (2015) A central role for the retrosplenial cortex in de novo
1049 environmental learning. *Elife* 4.
- 1050 Bainbridge WA, Hall EH, Baker CI (2020) Distinct Representational Structure and
1051 Localization for Visual Encoding and Recall during Visual Imagery. *Cerebral Cortex*
1052 00:1–16 Available at:
1053 http://fdslive.oup.com/www.oup.com/pdf/production_in_progress.pdf [Accessed
1054 December 7, 2020].
- 1055 Baldassano C, Esteva A, Fei-Fei L, Beck DM (2016) Two Distinct Scene-Processing Networks
1056 Connecting Vision and Memory. *eNeuro* 3 Available at:
1057 <http://www.ncbi.nlm.nih.gov/pubmed/27822493> [Accessed August 18, 2019].
- 1058 Barnett AJ, Reilly W, Dimsdale-Zucker HR, Mizrak E, Reagh Z, Ranganath C (2021) Intrinsic
1059 connectivity reveals functionally distinct cortico-hippocampal networks in the human
1060 brain. *PLoS Biol* 19:e3001275 Available at:
1061 <https://journals.plos.org/plosbiology/article?id=10.1371/journal.pbio.3001275>
1062 [Accessed April 17, 2024].
- 1063 Barry DN, Barnes GR, Clark IA, Maguire EA (2019) The Neural Dynamics of Novel Scene
1064 Imagery. *J Neurosci* 39:4375–4386 Available at:
1065 <http://www.ncbi.nlm.nih.gov/pubmed/30902867> [Accessed August 18, 2019].

- 1066 Baumann O, Mattingley JB (2010) Medial parietal cortex encodes perceived heading
1067 direction in humans. *Journal of Neuroscience* 30:12897–12901.
- 1068 Berens SC, Joensen BH, Horner AJ (2021) Tracking the Emergence of Location-based Spatial
1069 Representations in Human Scene-Selective Cortex. *J Cogn Neurosci* 33:445–462
1070 Available at: [https://direct.mit.edu/jocn/article/33/3/445/95543/Tracking-the-](https://direct.mit.edu/jocn/article/33/3/445/95543/Tracking-the-Emergence-of-Location-based-Spatial)
1071 [Emergence-of-Location-based-Spatial](https://direct.mit.edu/jocn/article/33/3/445/95543/Tracking-the-Emergence-of-Location-based-Spatial) [Accessed August 4, 2022].
- 1072 Bonner MF, Epstein RA (2017) Coding of navigational affordances in the human visual
1073 system. *Proc Natl Acad Sci U S A* 114:4793–4798 Available at:
1074 www.pnas.org/cgi/doi/10.1073/pnas.1618228114 [Accessed December 9, 2020].
- 1075 Braga RM, Buckner RL (2017) Parallel Interdigitated Distributed Networks within the
1076 Individual Estimated by Intrinsic Functional Connectivity. *Neuron* 95:457–471.e5.
- 1077 Brunec IK, Bellana B, Ozubko JD, Man V, Robin J, Liu ZX, Grady C, Rosenbaum RS, Winocur
1078 G, Barense MD, Moscovitch M (2018) Multiple Scales of Representation along the
1079 Hippocampal Anteroposterior Axis in Humans. *Current Biology* 28:2129–2135.e6.
- 1080 Buckner RL, Krienen FM, Castellanos A, Diaz JC, Thomas Yeo BT (2011) The organization of
1081 the human cerebellum estimated by intrinsic functional connectivity. *J Neurophysiol*
1082 106:2322–2345.
- 1083 Chen YY, Areti A, Yoshor D, Foster BL (2024) Perception and Memory Reinstatement Engage
1084 Overlapping Face-Selective Regions within Human Ventral Temporal Cortex. *The*
1085 *Journal of Neuroscience* 44:e2180232024 Available at:
1086 <http://www.jneurosci.org/content/44/22/e2180232024.abstract>.
- 1087 Chrastil ER, Tobyne SM, Nauer RK, Chang AE, Stern CE (2018) Converging meta-analytic and
1088 connectomic evidence for functional subregions within the human retrosplenial region.
1089 *Behavioral Neuroscience* 132:339–355 Available at: [/record/2018-51215-002](https://doi.org/10.1037/bne0000202)
1090 [Accessed November 4, 2020].
- 1091 Christiaan Klink P, Chen X, Vanduffel W, Roelfsema PR (2021) Population receptive fields in
1092 non-human primates from whole-brain fmri and large-scale neurophysiology in visual
1093 cortex. *Elife* 10.
- 1094 Cooper RA, Ritchey M (2019) Cortico-hippocampal network connections support the
1095 multidimensional quality of episodic memory. *Elife* 8.
- 1096 Cox RW (1996) AFNI: Software for analysis and visualization of functional magnetic
1097 resonance neuroimages. *Computers and Biomedical Research* 29:162–173.

- 1098 Dale AM, Fischl B, Sereno MI (1999) Cortical surface-based analysis: I. Segmentation and
1099 surface reconstruction. *Neuroimage* 9:179–194.
- 1100 Dilks DD, Julian JB, Paunov AM, Kanwisher N (2013) The occipital place area is causally and
1101 selectively involved in scene perception. *Journal of Neuroscience* 33:1331–1336.
- 1102 Dilks DD, Kamps FS, Persichetti AS (2022) Three cortical scene systems and their
1103 development. *Trends Cogn Sci* 26:117–127 Available at:
1104 <http://www.cell.com/article/S1364661321002874/fulltext> [Accessed January 17,
1105 2022].
- 1106 DiNicola LM, Braga RM, Buckner RL (2020) Parallel distributed networks dissociate episodic
1107 and social functions within the individual. *J Neurophysiol* 123:1144–1179 Available at:
1108 <https://journals.physiology.org/doi/10.1152/jn.00529.2019> [Accessed March 19, 2020].
- 1109 DiNicola LM, Buckner RL (2021) Precision estimates of parallel distributed association
1110 networks: evidence for domain specialization and implications for evolution and
1111 development. *Curr Opin Behav Sci* 40:120–129 Available at:
1112 <https://linkinghub.elsevier.com/retrieve/pii/S2352154621000772> [Accessed May 18,
1113 2021].
- 1114 Dixon ML, Andrews-Hanna JR, Spreng RN, Irving ZC, Mills C, Girn M, Christoff K (2017)
1115 Interactions between the default network and dorsal attention network vary across
1116 default subsystems, time, and cognitive states. *Neuroimage* 147:632–649 Available at:
1117 <https://www.sciencedirect.com/science/article/pii/S1053811916307996>.
- 1118 Draschkow D, Nobre AC, van Ede F (2022) Multiple spatial frames for immersive working
1119 memory. *Nature Human Behaviour* 2022 6:4 6:536–544 Available at:
1120 <https://www.nature.com/articles/s41562-021-01245-y> [Accessed June 6, 2022].
- 1121 Du J, DiNicola LM, Angeli PA, Saadon-Grosman N, Sun W, Kaiser S, Ladopoulou J, Xue A, Yeo
1122 BTT, Eldaief MC, Buckner RL (2024) Organization of the human cerebral cortex
1123 estimated within individuals: networks, global topography, and function. *J Neurophysiol*
1124 131:1014–1082 Available at: <https://doi.org/10.1152/jn.00308.2023>.
- 1125 DuPre E et al. (2021) TE-dependent analysis of multi-echo fMRI with *tedana*. *J Open Source*
1126 *Softw* 6:3669 Available at: <https://joss.theoj.org/papers/10.21105/joss.03669>
1127 [Accessed June 26, 2022].
- 1128 DuPre E, Salo T, Markello R, Kundu P, Whitaker K, Handwerker D (2019) ME-ICA/tedana: 0.0.6.
1129 Available at: <https://zenodo.org/record/2558498> [Accessed February 7, 2020].

- 1130 Epstein R, Kanwisher N (1998) A cortical representation the local visual environment. *Nature*
1131 392:598–601.
- 1132 Epstein RA, Baker CI (2019) Scene Perception in the Human Brain. *Annu Rev Vis Sci*
1133 5:annurev-vision-091718-014809 Available at:
1134 <https://www.annualreviews.org/doi/10.1146/annurev-vision-091718-014809>
1135 [Accessed July 28, 2019].
- 1136 Epstein RA, Higgins JS, Jablonski K, Feiler AM (2007) Visual Scene Processing in Familiar and
1137 Unfamiliar Environments. *J Neurophysiol* 97:3670–3683 Available at:
1138 <https://www.physiology.org/doi/10.1152/jn.00003.2007> [Accessed April 22, 2020].
- 1139 Evans JW, Kundu P, Horovitz SG, Bandettini PA (2015) Separating slow BOLD from non-BOLD
1140 baseline drifts using multi-echo fMRI. *Neuroimage* 105:189–197.
- 1141 Favila SE, Lee H, Kuhl BA (2020) Transforming the Concept of Memory Reactivation. *Trends*
1142 *Neurosci* 43:939–950.
- 1143 Fischl B (2012) FreeSurfer. *Neuroimage* 62:774–781.
- 1144 Fischl B, Salat DH, Busa E, Albert M, Dieterich M, Haselgrove C, Van Der Kouwe A, Killiany R,
1145 Kennedy D, Klaveness S, Montillo A, Makris N, Rosen B, Dale AM (2002) Whole brain
1146 segmentation: Automated labeling of neuroanatomical structures in the human brain.
1147 *Neuron* 33:341–355.
- 1148 Foster BL, Koslov SR, Aponik-Gremillion L, Monko ME, Hayden BY, Heilbronner SR (2023) A
1149 tripartite view of the posterior cingulate cortex. *Nat Rev Neurosci* 24:173–189 Available
1150 at: <https://doi.org/10.1038/s41583-022-00661-x>.
- 1151 Fox MD, Corbetta M, Snyder AZ, Vincent JL, Raichle ME (2006) Spontaneous neuronal activity
1152 distinguishes human dorsal and ventral attention systems. *Proceedings of the National*
1153 *Academy of Sciences* 103:10046–10051 Available at:
1154 <https://doi.org/10.1073/pnas.0604187103>.
- 1155 Fox MD, Snyder AZ, Vincent JL, Corbetta M, Van Essen DC, Raichle ME (2005) The human
1156 brain is intrinsically organized into dynamic, anticorrelated functional networks. *Proc*
1157 *Natl Acad Sci U S A* 102:9673–9678 Available at:
1158 <https://pubmed.ncbi.nlm.nih.gov/15976020/> [Accessed July 13, 2022].
- 1159 Gilmore AW, Nelson SM, McDermott KB (2015) A parietal memory network revealed by
1160 multiple MRI methods. *Trends Cogn Sci* 19:534–543 Available at:
1161 <https://www.sciencedirect.com/science/article/pii/S1364661315001552> [Accessed
1162 June 18, 2019].

- 1163 Gilmore AW, Nelson SM, McDermott KB (2016) The Contextual Association Network
1164 Activates More for Remembered than for Imagined Events. *Cerebral Cortex* 26:611–617
1165 Available at: <http://www.nil.wustl.edu/> [Accessed November 4, 2020].
- 1166 Glasser MF, Coalson TS, Robinson EC, Hacker CD, Harwell J, Yacoub E, Ugurbil K, Andersson
1167 J, Beckmann CF, Jenkinson M, Smith SM, Van Essen DC (2016) A multi-modal
1168 parcellation of human cerebral cortex. *Nature* 536:171–178 Available at:
1169 <http://balsa.wustl.edu/WN56>. [Accessed November 5, 2020].
- 1170 Gomez J, Barnett M, Grill-Spector K (2019) Extensive childhood experience with Pokémon
1171 suggests eccentricity drives organization of visual cortex. *Nature Human Behaviour*
1172 2019:1 Available at: <https://www.nature.com/articles/s41562-019-0592-8> [Accessed
1173 May 5, 2019].
- 1174 Gordon EM et al. (2017) Precision Functional Mapping of Individual Human Brains. *Neuron*
1175 95:791-807.e7.
- 1176 Gratton C, Laumann TO, Nielsen AN, Greene DJ, Gordon EM, Gilmore AW, Nelson SM,
1177 Coalson RS, Snyder AZ, Schlaggar BL, Dosenbach NUF, Petersen SE (2018) Functional
1178 Brain Networks Are Dominated by Stable Group and Individual Factors, Not Cognitive or
1179 Daily Variation. *Neuron* 98:439-452.e5.
- 1180 Grill-Spector K, Weiner KS (2014) The functional architecture of the ventral temporal cortex
1181 and its role in categorization. *Nat Rev Neurosci* 15:536–548 Available at:
1182 </pmc/articles/PMC4143420/?report=abstract> [Accessed July 1, 2020].
- 1183 Haskins AJ, Mentch J, Botch TL, Robertson CE (2020) Active vision in immersive, 360° real-
1184 world environments. *Scientific Reports* 2020 10:1 10:1–11 Available at:
1185 <https://www.nature.com/articles/s41598-020-71125-4> [Accessed January 19, 2022].
- 1186 Hasson U, Harel M, Levy I, Malach R (2003) Large-scale mirror-symmetry organization of
1187 human occipito-temporal object areas. *Neuron* 37:1027–1041 Available at:
1188 <https://pubmed.ncbi.nlm.nih.gov/12670430/> [Accessed November 4, 2020].
- 1189 Henriksson L, Mur M, Kriegeskorte N (2019) Rapid Invariant Encoding of Scene Layout in
1190 Human OPA. *Neuron* Available at:
1191 <https://www.sciencedirect.com/science/article/pii/S0896627319303496> [Accessed
1192 May 14, 2019].
- 1193 Huntenburg JM, Bazin PL, Margulies DS (2018) Large-Scale Gradients in Human Cortical
1194 Organization. *Trends Cogn Sci* 22:21–31 Available at:
1195 <http://www.cell.com/article/S1364661317302401/fulltext> [Accessed June 21, 2022].

- 1196 Jo HJ, Gotts SJ, Reynolds RC, Bandettini PA, Martin A, Cox RW, Saad ZS (2013) Effective
1197 Preprocessing Procedures Virtually Eliminate Distance-Dependent Motion Artifacts in
1198 Resting State fMRI. *J Appl Math* 2013 Available at: </pmc/articles/PMC3886863/>
1199 [Accessed June 21, 2022].
- 1200 Julian JB, Fedorenko E, Webster J, Kanwisher N (2012) An algorithmic method for functionally
1201 defining regions of interest in the ventral visual pathway. Available at:
1202 <http://web.mit.edu/bcs/nklab/GSS.shtml> [Accessed January 20, 2022].
- 1203 Julian JB, Ryan J, Hamilton RH, Epstein RA (2016) The Occipital Place Area Is Causally
1204 Involved in Representing Environmental Boundaries during Navigation. *Current Biology*
1205 26:1104–1109 Available at: [https://www.cell.com/current-biology/fulltext/S0960-](https://www.cell.com/current-biology/fulltext/S0960-9822(16)30177-4)
1206 9822(16)30177-4 [Accessed May 15, 2019].
- 1207 Kamps FS, Julian JB, Kubilius J, Kanwisher N, Dilks DD (2016) The occipital place area
1208 represents the local elements of scenes. *Neuroimage* 132:417–424.
- 1209 Kanwisher N (2017) The Quest for the FFA and Where It Led. *The Journal of Neuroscience*
1210 37:1056 Available at: <http://www.jneurosci.org/content/37/5/1056.abstract>.
- 1211 Kanwisher N, McDermott J, Chun MM (1997) The fusiform face area: A module in human
1212 extrastriate cortex specialized for face perception. *Journal of Neuroscience* 17:4302–
1213 4311 Available at: <https://www.jneurosci.org/content/17/11/4302> [Accessed May 18,
1214 2021].
- 1215 Kiyonaga A, Scimeca JM, Bliss DP, Whitney D (2017) Serial dependence across perception,
1216 attention, and memory. *Trends Cogn Sci* 21:493 Available at:
1217 </pmc/articles/PMC5516910/> [Accessed July 17, 2022].
- 1218 Kong R, Yang Q, Gordon E, Xue A, Yan X, Orban C, Zuo X-N, Spreng N, Ge T, Holmes A, Eickhoff
1219 S, Yeo BTT (2021) Individual-Specific Areal-Level Parcellations Improve Functional
1220 Connectivity Prediction of Behavior. *Cerebral Cortex* 31:4477–4500 Available at:
1221 <https://doi.org/10.1093/cercor/bhab101>.
- 1222 Kundu P, Inati SJ, Evans JW, Luh WM, Bandettini PA (2012) Differentiating BOLD and non-
1223 BOLD signals in fMRI time series using multi-echo EPI. *Neuroimage* 60:1759–1770.
- 1224 Laumann TO, Gordon EM, Adeyemo B, Snyder AZ, Joo SJ, Chen MY, Gilmore AW, McDermott
1225 KB, Nelson SM, Dosenbach NUF, Schlaggar BL, Mumford JA, Poldrack RA, Petersen SE
1226 (2015) Functional System and Areal Organization of a Highly Sampled Individual Human
1227 Brain. *Neuron* 87:657–670.

- 1228 Lescroart MD, Gallant JL (2019) Human Scene-Selective Areas Represent 3D Configurations
1229 of Surfaces. *Neuron* 101:178-192.e7.
- 1230 Libby A, Buschman TJ (2021) Rotational dynamics reduce interference between sensory and
1231 memory representations. *Nature Neuroscience* 2021 24:5 24:715–726 Available at:
1232 <https://www.nature.com/articles/s41593-021-00821-9> [Accessed April 16, 2024].
- 1233 Maguire EA, Burgess N, Donnett JG, Frackowiak RSJ, Frith CD, O’Keefe J (1998) Knowing
1234 where and getting there: A human navigation network. *Science* (1979) 280:921–924
1235 Available at: <https://pubmed.ncbi.nlm.nih.gov/9572740/> [Accessed November 4,
1236 2020].
- 1237 Marchette SA, Vass LK, Ryan J, Epstein RA (2014) Anchoring the neural compass: Coding of
1238 local spatial reference frames in human medial parietal lobe. *Nat Neurosci* 17:1598–
1239 1606 Available at:
1240 [https://static1.squarespace.com/static/55aaa148e4b0ba360335ef21/t/55b07091e4b
1241 0dd22812a8c37/1437626513802/Marchette-2014-Nature-Neuro.pdf](https://static1.squarespace.com/static/55aaa148e4b0ba360335ef21/t/55b07091e4b0dd22812a8c37/1437626513802/Marchette-2014-Nature-Neuro.pdf) [Accessed May
1242 13, 2019].
- 1243 Marchette SA, Vass LK, Ryan J, Epstein RA (2015) Outside looking in: Landmark
1244 generalization in the human navigational system. *Journal of Neuroscience* 35:14896–
1245 14908.
- 1246 Margulies DS, Ghosh SS, Goulas A, Falkiewicz M, Huntenburg JM, Langs G, Bezgin G, Eickhoff
1247 SB, Castellanos FX, Petrides M, Jefferies E, Smallwood J (2016) Situating the default-
1248 mode network along a principal gradient of macroscale cortical organization. *Proc Natl
1249 Acad Sci U S A* 113:12574–12579.
- 1250 Murphy C, Jefferies E, Rueschemeyer SA, Sormaz M, Wang H ting, Margulies DS, Smallwood
1251 J (2018) Distant from input: Evidence of regions within the default mode network
1252 supporting perceptually-decoupled and conceptually-guided cognition. *Neuroimage*
1253 171:393–401.
- 1254 Murphy C, Wang H-T, Konu D, Lowndes R, Margulies DS, Jefferies E, Smallwood J (2019)
1255 Modes of operation: A topographic neural gradient supporting stimulus dependent and
1256 independent cognition. *Neuroimage* 186:487–496 Available at:
1257 <https://doi.org/10.1016/j.neuroimage.2018.11.009> [Accessed June 17, 2019].
- 1258 Nau M, Navarro Schröder T, Frey M, Doeller CF (2020) Behavior-dependent directional tuning
1259 in the human visual-navigation network. *Nat Commun* 11:3247 Available at:
1260 <http://www.nature.com/articles/s41467-020-17000-2> [Accessed December 6, 2020].

- 1261 Park S, Intraub H, Yi D-J, Widders D, Chun MM (2007) Beyond the Edges of a View: Boundary
1262 Extension in Human Scene-Selective Visual Cortex. *Neuron* 54:335–342 Available at:
1263 <https://www.sciencedirect.com/science/article/pii/S0896627307002565> [Accessed
1264 April 28, 2019].
- 1265 Persichetti AS, Dilks DD (2016) Perceived egocentric distance sensitivity and invariance
1266 across scene-selective cortex. *Cortex* 77:155–163.
- 1267 Persichetti AS, Dilks DD (2019) Distinct representations of spatial and categorical
1268 relationships across human scene-selective cortex. *Proceedings of the National
1269 Academy of Sciences*:201903057 Available at:
1270 <http://www.pnas.org/lookup/doi/10.1073/pnas.1903057116> [Accessed October 1,
1271 2019].
- 1272 Power JD, Cohen AL, Nelson SM, Wig GS, Barnes KA, Church JA, Vogel AC, Laumann TO,
1273 Miezin FM, Schlaggar BL, Petersen SE (2011) Functional Network Organization of the
1274 Human Brain. *Neuron* 72:665–678.
- 1275 Raichle ME, MacLeod AM, Snyder AZ, Powers WJ, Gusnard DA, Shulman GL (2001) A default
1276 mode of brain function. *Proceedings of the National Academy of Sciences* 98:676–682
1277 Available at: <https://doi.org/10.1073/pnas.98.2.676>.
- 1278 Ranganath C, Ritchey M (2012) Two cortical systems for memory-guided behaviour. *Nat Rev
1279 Neurosci* 13:713–726.
- 1280 Reagh ZM, Ranganath C (2018) What does the functional organization of cortico-
1281 hippocampal networks tell us about the functional organization of memory? *Neurosci
1282 Lett* 680:69–76 Available at:
1283 <https://www.sciencedirect.com/science/article/pii/S0304394018303136>.
- 1284 Reagh ZM, Ranganath C (2023) Flexible reuse of cortico-hippocampal representations
1285 during encoding and recall of naturalistic events. *Nature Communications* 2023 14:1
1286 14:1–15 Available at: <https://www.nature.com/articles/s41467-023-36805-5> [Accessed
1287 April 17, 2024].
- 1288 Reznik D, Margulies DS, Witter MP, Doeller CF (2024) Evidence for convergence of distributed
1289 cortical processing in band-like functional zones in human entorhinal cortex. *Current
1290 Biology* 34:5457–5469.e2 Available at: <https://doi.org/10.1016/j.cub.2024.10.020>.
- 1291 Ritchey M, Cooper RA (2020) Deconstructing the Posterior Medial Episodic Network. *Trends
1292 Cogn Sci* xx Available at: <https://doi.org/10.1016/j.tics.2020.03.006> [Accessed April 25,
1293 2020].

- 1294 Ritchey M, Libby LA, Ranganath C (2015) Cortico-hippocampal systems involved in memory
1295 and cognition: the PMAT framework 3. Available at:
1296 <http://dx.doi.org/10.1016/bs.pbr.2015.04.001> [Accessed September 2, 2019].
- 1297 Robertson CE, Hermann KL, Mynick A, Kravitz DJ, Kanwisher N (2016) Neural
1298 Representations Integrate the Current Field of View with the Remembered 360°
1299 Panorama in Scene-Selective Cortex. *Current Biology* 26:2463–2468 Available at:
1300 <https://www.sciencedirect.com/science/article/pii/S0960982216307539> [Accessed
1301 April 8, 2019].
- 1302 Rosenke M, van Hoof R, van den Hurk J, Grill-Spector K, Goebel R (2021) A Probabilistic
1303 Functional Atlas of Human Occipito-Temporal Visual Cortex. *Cerebral Cortex* 31:603–
1304 619 Available at: <https://doi.org/10.1093/cercor/bhaa246>.
- 1305 Rust NC, Palmer SE (2021) Remembering the Past to See the Future.
1306 <https://doi.org/101146/annurev-vision-093019-112249> 7 Available at:
1307 <https://www.annualreviews.org/doi/abs/10.1146/annurev-vision-093019-112249>
1308 [Accessed September 7, 2021].
- 1309 Saad ZS, Reynolds RC (2012) SUMA. *Neuroimage* 62:768–773.
- 1310 Silson EH, Gilmore AW, Kalinowski SE, Steel A, Kidder A, Martin A, Baker CI (2018) A
1311 posterior-anterior distinction between scene perception and scene construction in
1312 human medial parietal cortex. *Journal of Neuroscience* 39:705–717 Available at:
1313 <https://www.jneurosci.org/content/early/2018/11/30/JNEUROSCI.1219-18.2018>
1314 [Accessed September 21, 2021].
- 1315 Silson EH, McKeefry DJ, Rodgers J, Gouws AD, Hymers M, Morland AB (2013) Specialized and
1316 independent processing of orientation and shape in visual field maps LO1 and LO2. *Nat*
1317 *Neurosci* 16:267–269 Available at: <https://doi.org/10.1038/nn.3327>.
- 1318 Silson EH, Steel A, Kidder A, Gilmore AW, Baker CI (2019) Distinct subdivisions of human
1319 medial parietal cortex support recollection of people and places. *Elife* 8.
- 1320 Silson EH, Steel AD, Baker CI (2016) Scene-Selectivity and Retinotopy in Medial Parietal
1321 Cortex. *Front Hum Neurosci* 10:412 Available at:
1322 <http://journal.frontiersin.org/Article/10.3389/fnhum.2016.00412/abstract> [Accessed
1323 April 8, 2019].
- 1324 Srokova S, Hill PF, Rugg MD (2022) The Retrieval-related Anterior shift is Moderated by Age
1325 and Correlates with Memory Performance. *Journal of Neuroscience:JN-RM-1763-21*
1326 Available at: [https://www.jneurosci.org/content/early/2022/01/06/JNEUROSCI.1763-
1327 21.2021](https://www.jneurosci.org/content/early/2022/01/06/JNEUROSCI.1763-21.2021) [Accessed January 17, 2022].

- 1328 Steel A, Angeli PA, Silson EH, Robertson CE (2024a) Retinotopic coding organizes the
1329 interaction between internally and externally oriented brain networks.
1330 bioRxiv:2024.09.25.615084 Available at:
1331 <http://biorxiv.org/content/early/2024/11/04/2024.09.25.615084.abstract>.
- 1332 Steel A, Billings MM, Silson EH, Robertson CE (2021) A network linking scene perception and
1333 spatial memory systems in posterior cerebral cortex. *Nature Communications* 2021
1334 12:1 12:1–13 Available at: <https://doi.org/10.1038/s41467-021-22848-z> [Accessed May
1335 18, 2021].
- 1336 Steel A, Garcia BD, Goyal K, Mynick A, Robertson CE (2023) Scene Perception and
1337 Visuospatial Memory Converge at the Anterior Edge of Visually Responsive Cortex. *The*
1338 *Journal of Neuroscience* 43:5723 Available at:
1339 <http://www.jneurosci.org/content/43/31/5723.abstract>.
- 1340 Steel A, Garcia BD, Silson EH, Robertson CE (2022) Evaluating the efficacy of multi-echo ICA
1341 denoising on model-based fMRI. *Neuroimage* 264:119723.
- 1342 Steel A, Silson EH, Garcia BD, Robertson CE (2024b) A retinotopic code structures the
1343 interaction between perception and memory systems. *Nat Neurosci* 27:339–347
1344 Available at: <https://doi.org/10.1038/s41593-023-01512-3>.
- 1345 Steel A, Thomas C, Trefler A, Chen G, Baker CI (2019) Finding the baby in the bath water –
1346 evidence for task-specific changes in resting state functional connectivity evoked by
1347 training. *Neuroimage* 188:524–538.
- 1348 Stigliani A, Weiner KS, Grill-Spector K (2015) Temporal Processing Capacity in High-Level
1349 Visual Cortex Is Domain Specific. *The Journal of Neuroscience* 35:12412 Available at:
1350 <http://www.jneurosci.org/content/35/36/12412.abstract>.
- 1351 Summerfield C, De Lange FP (2014) Expectation in perceptual decision making: neural and
1352 computational mechanisms. *Nat Rev Neurosci* 15:745–756 Available at:
1353 <https://pubmed.ncbi.nlm.nih.gov/25315388/> [Accessed July 17, 2022].
- 1354 Szinte M, Knapen T (2020) Visual Organization of the Default Network. *Cerebral Cortex*
1355 30:3518–3527 Available at:
1356 <https://academic.oup.com/cercor/article/30/6/3518/5685762> [Accessed July 13,
1357 2022].
- 1358 Thomas Yeo BT, Krienen FM, Sepulcre J, Sabuncu MR, Lashkari D, Hollinshead M, Roffman
1359 JL, Smoller JW, Zöllei L, Polimeni JR, Fisch B, Liu H, Buckner RL (2011) The organization
1360 of the human cerebral cortex estimated by intrinsic functional connectivity. *J*
1361 *Neurophysiol* 106:1125–1165.

- 1362 Vass LK, Epstein RA (2013) Abstract Representations of Location and Facing Direction in the
1363 Human Brain. *Journal of Neuroscience* 33:6133–6142 Available at:
1364 <https://www.jneurosci.org/content/33/14/6133> [Accessed April 13, 2022].
- 1365 Vass LK, Epstein RA (2017) Common Neural Representations for Visually Guided
1366 Reorientation and Spatial Imagery. *Cerebral Cortex* 27:1457–1471 Available at:
1367 <https://dx.doi.org/10.1093/cercor/bhv343> [Accessed April 17, 2024].
- 1368 Wandell BA, Dumoulin SO, Brewer AA (2007) Visual field maps in human cortex. *Neuron*
1369 56:366–383 Available at: <https://pubmed.ncbi.nlm.nih.gov/17964252/> [Accessed July
1370 13, 2022].
- 1371 Wang L, Mruczek REB, Arcaro MJ, Kastner S (2015) Probabilistic maps of visual topography
1372 in human cortex. *Cerebral Cortex* 25:3911–3931 Available at:
1373 </pmc/articles/PMC4585523/?report=abstract> [Accessed November 4, 2020].
- 1374 Weiner KS, Barnett MA, Witthoft N, Golarai G, Stigliani A, Kay KN, Gomez J, Natu VS, Amunts
1375 K, Zilles K, Grill-Spector K (2018) Defining the most probable location of the
1376 parahippocampal place area using cortex-based alignment and cross-validation.
1377 *Neuroimage* 170:373–384 Available at: <https://pubmed.ncbi.nlm.nih.gov/28435097/>
1378 [Accessed November 4, 2020].
- 1379 Weiskopf N, Hutton C, Josephs O, Deichmann R (2006) Optimal EPI parameters for reduction
1380 of susceptibility-induced BOLD sensitivity losses: A whole-brain analysis at 3 T and 1.5
1381 T.
- 1382 Willbrand EH, Tsai Y-H, Gagnant T, Weiner KS (2024) Updating the sulcal landscape of the
1383 human lateral parieto-occipital junction provides anatomical, functional, and cognitive
1384 insights. Available at: <http://dx.doi.org/10.7554/eLife.90451.2>.
- 1385 Yeo BTT, Krienen FM, Eickhoff SB, Yaakub SN, Fox PT, Buckner RL, Asplund CL, Chee MWL
1386 (2015) Functional Specialization and Flexibility in Human Association Cortex. *Cerebral*
1387 *Cortex* 25:3654–3672 Available at: <https://doi.org/10.1093/cercor/bhu217>.
- 1388
- 1389